POLITECNICO
MILANO 1863

SCUOLA DI INGEGNERIA INDUSTRIALE
E DELL'INFORMAZIONE

# Automatic measurement of airway dimensions from CT images in health and asthma

TESI DI LAUREA MAGISTRALE IN
BIOMEDICAL ENGINEERING - INGEGNERIA BIOMEDICA

Author: Claudia Mascheroni

Student ID: 10563437
Advisor: Prof. Andrea Aliverti
Co-advisor: Francesca Pennati, PhD
Academic Year: 2021-22

# Acknowledgments

I express sincere appreciation to my advisor Professor Andrea Aliverti for his availability and for giving me the opportunity to work on this thesis under the supervision of Francesca Pennati. Her guidance and precious advices were fundamental and I cannot thank her enough for helping me facing the problem encountered along the way.

Many thanks also to my friends and fellow adventurers, Franci, Jessie and Alice, for keeping my spirits and motivation high during this journey.

Words cannot express my gratitude to my parents, my mother Katia and my father Carlo, for their limitless support, patience and encouragement. If they had not helped me out, I would have never succeed.

# Abstract

An increase in respiratory diseases has been estimated in recent years and one of the main contributors is air pollution [49]. Among these pathologies, one of the most widespread and common is asthma, affecting more than 300 million people worldwide [50]. Asthma is an obstructive disease, characterized by structural changes of the airways, including thickening of the bronchial wall and narrowing of the lumen. The combination of these modifications is called airway remodelling. The analysis of this phenomenon is fundamental to evaluate disease progression and to develop new therapeutic treatments to attenuate or reverse these structural changes [52]. In this sense, computed tomography (CT) offers the possibility to qualitatively and quantitatively assess airway morphology, thus it can be used to diagnose and monitor disease progression [53].

The aim of the thesis is to develop an automatic algorithm for the segmentation of the airways and the accurate measurement of morphological parameters on CT images. The algorithm was implemented and hardened starting from the processing of CT images of healthy subjects and, after its validation, it was applied to CT images of asthmatic patients, to evaluate the alterations induced by disease.

The work consists of three main phases: the implementation of the algorithm, its validation, the application of the algorithm in health and asthma.

Airways were segmented based on a region growing algorithm. The centreline was extracted and the section orthogonal to the centreline is reconstructed in specific points for performing the measurements. Starting from the bifurcation points of the centreline, a suitable data structure was created to organize and store the measurements of individual branches. Finally, a morphometric analysis was conducted through the identification and the computation of relevant morphological parameters. The algorithm was validated by comparing the measurements to the

ones obtained with manual measurements and was applied to CT images of healthy and asthmatic subjects to quantify the structural changes occurring with disease.

The validation results demonstrate a good correlation and a low difference with manual measurements. Errors have been observed especially in correspondence of the small airways, for which a strategy for future improvement has been proposed. The comparison between health and asthma revealed a narrowing of the lumen and a thickening of the bronchial wall in the disease. Finally, an insight was reported on how the tool developed in this work can potentially be used to study the structure-function relationship in lung disease, by investigating the relationship between structural measurements and abnormalities observed on magnetic resonance images with hyperpolarized Helium-3 gas.

In conclusion, the implemented algorithm represents a valid and innovative tool for the quantitative analysis of the airways. The morphological parameters identified were successfully validated and structural alterations were quantified in asthma.

However, the method presents some critical issues. The algorithm for extracting the central axis can be improved, to increase the number of generations identified through segmentation. A validation procedure on the identification of the bifurcation points, at the basis of the creation of the data structure, is still missing. Furthermore, the algorithm was tested on a limited number of subjects, thus it may not be sufficiently robust to account for the inter-subject airways' variability.

In a long-term perspective and after further improvements, this tool could support clinicians in diagnosis, follow-up and definition of treatment plan.

**Key-words:** asthma, airways remodelling, CT-imaging, segmentation, morphometry analysis

# Sommario

Negli ultimi anni è stato stimato un aumento delle malattie a carico del sistema respiratorio e una delle cause principali è l'inquinamento atmosferico [49]. Tra queste patologie, una delle più diffuse e comuni, è l'asma che colpisce più di 300 milioni di persone in tutto il mondo [50]. L'asma è una malattia ostruttiva, caratterizzata da alterazioni strutturali delle vie aeree, quali l'ispessimento della parete bronchiale e il restringimento del lume. La combinazione di queste alterazioni è chiamata rimodellamento delle vie aeree. L'analisi di questo fenomeno è fondamentale per valutare la progressione della malattia e per sviluppare nuovi trattamenti terapeutici in modo da attenuare o invertire questi cambiamenti strutturali [52]. Per tale scopo, la tomografia assiale computerizzata (TAC) offre la possibilità di valutare qualitativamente e quantitativamente la morfologia delle vie aeree, e quindi può essere utilizzata per diagnosticare e monitorare la progressione della malattia [53].

Lo scopo della tesi è sviluppare un algoritmo automatico per la segmentazione delle vie aeree e l'accurata misurazione di parametri morfologici su immagini TAC. L'algoritmo è stato implementato e irrobustito a partire dall'elaborazione di immagini TAC di soggetti sani e, dopo la sua validazione, è stato applicato a immagini TAC di pazienti asmatici, per valutare le alterazioni indotte dalla malattia.

Il lavoro si compone di tre fasi principali: l'implementazione dell'algoritmo, la sua validazione, l'applicazione dell'algoritmo a soggetti sani ed asmatici.

Le vie aeree sono state segmentate utilizzando un algoritmo di region growing. Da cui si è estratta l'asse centrale e la sezione ortogonale a tale asse è stata ricostruita in punti specifici per effettuare le misure. A partire dai punti di biforcazione individuati sull'asse centrale, si è creata un'apposita struttura dati per organizzare e

memorizzare le misure dei singoli rami. Infine, è stata condotta un'analisi morfometrica attraverso l'identificazione e il calcolo dei parametri morfologici rilevanti. L'algoritmo è stato validato confrontando tali misurazioni con misurazioni ottenute manualmente ed è stato poi applicato a immagini TAC di soggetti sani e asmatici per quantificare i cambiamenti strutturali che si verificano in presenza della malattia.

I risultati della validazione dimostrano una buona correlazione e una bassa differenza con le misurazioni manuali. Si sono osservati errori di misura soprattutto in corrispondenza delle piccole vie aeree, per le quali è stata proposta una strategia per un miglioramento futuro. Il confronto tra sani e asmatici ha rivelato un restringimento del lume e un ispessimento della parete bronchiale nei patologici. Infine, è stato riportato un approfondimento su come lo strumento sviluppato in questo lavoro possa potenzialmente essere utilizzato per studiare la relazione struttura-funzione nelle malattie polmonari, indagando la relazione tra le misurazioni strutturali e anomalie osservate in immagini di risonanza magnetica con gas Helium-3 iperpolarizzato.

In conclusione, l'algoritmo implementato rappresenta un valido ed innovativo strumento per l'analisi quantitativa delle vie aeree. I parametri morfologici identificati sono stati validati con successo e sono state quantificate alterazioni strutturali nelle vie aeree di pazienti asmatici.

Tuttavia, il metodo presenta alcune criticità. L'algoritmo per l'estrazione dell'asse centrale può essere migliorato, per aumentare il numero di generazioni identificate attraverso la segmentazione. Manca ancora una procedura di validazione relativa all’identificazione dei punti di biforcazione, alla base della creazione della struttura dati. Inoltre, l'algoritmo è stato testato su un numero limitato di soggetti, quindi potrebbe non essere sufficientemente robusto per tenere conto della variabilità delle vie aeree tra soggetti.

In una prospettiva a lungo termine e dopo ulteriori miglioramenti, questo strumento potrebbe supportare i medici nella diagnosi, nel follow-up e nella definizione di piani di trattamento.

**Parole chiave:** asma, rimodellamento delle vie aeree, immagini TAC, segmentazione, analisi morfometriche

# Content

# Motivation and aim of the work

Lung airways are conductive structure designated for gas exchange between the human body and the external environment[17]. For this reason, they are directly exposed to all the particles contained in the breathed air, including dust, soot, and also viruses, bacteria, pollutants, allergens which settle on the airways surface and so may lead to the development of respiratory disease[17]. Every individual may be affected by this kind of disease, although the risk increases with smoking and prolonged exposure to pollution. In recent years, there has been an overall increase in the prevalence of respiratory diseases worldwide and one of the major contributing factors to this trend is air pollution[49]. Among respiratory disease, asthma is one of the most common.

Asthma counts more than 300 million of affected individuals in the world[50] and can seriously compromise the life of people affected by it due to the recurrent symptoms caused such as wheezing and breathlessness, which, if worsened, can be fatal.

In order to preserve patients' quality of life, clinicians need to accurately diagnose their condition and appropriately manage patients through the long course of their illness[51].

In this sense, Computed Tomography (CT) imaging represents a useful tool for an accurate diagnosis of airways pathology as asthma in a non-invasive way.

Indeed, airways of patients affected by asthma present structural changes with respect to healthy ones that can be detected on CT images. This change in the morphological structure is called airway remodelling and the analysis of this phenomenon is necessary to obtain a correct diagnosis or to monitor the progression

of the disease and so design an effective treatment plan suitable for that specific patient[15][52].

First of all, CT images need to be processed with suitable algorithms designed to extract and accurately measure relevant morphological parameters related to airways geometry.

Although there are already available algorithms which perform the morphology analysis of human airways, there is still ongoing research in this field for several reasons: an accurate morphology analysis of human airways is crucial for obtaining reliable results and so there is a constant need for developing new algorithms that improve the accuracy and precision of the measurements; moreover, morphology analysis of human airways is not limited to research application but has a relevant implication in the clinical practice, as diagnosis, monitoring and treatment of respiratory disease[10][17][21].

This master thesis project fits into this topic. The objective is the development of a new algorithm for the extraction and accurate measurements of morphological airways parameters. At first, CT images of healthy subjects are processed with the implemented algorithm and the retrieved measurements are compared with measurements manually obtained in order to validate the algorithm. Then the algorithm is applied also to CT images of asthmatic patients and the airways structural differences among the two groups are investigated. Finally, an insight is reported about the structure-function relationship in lung diseases, assessed by comparing the quantitative data obtained from the developed tool and functional information depicted on hyperpolarized Helium-3 gas MRI, which represents the new frontier of research in the investigation of regional patterns of airflow obstruction in the lungs in an absolutely non-invasive way [27][54].

This thesis work is organised as follow: the introduction (Chapter 1) briefly describes the anatomy of the respiratory system, the usefulness of CT imaging for the analysis of airway morphometry and the findings of previous analogous works. Material and methods (Chapter 2) describes the procedure developed to achieve the project purpose. It can be divided into three main sections: the first section describes the steps followed to implement the algorithm which allows to extract and measure the relevant airways morphological parameters; the second section describes the procedure performed to validate the algorithm; the third section describes the comparison made between asthmatic and healthy (control) subjects, in particular, CT images of these two groups are processed with the validated algorithm and the measurements thus retrieved are compared in order to investigate the occurring structural changes among airways. Chapter 3 describes the results obtained from the three aforementioned sections. It is also reported a detailed description and interpretation of these results, combined with an explanation of errors and limitations that was found. Finally, chapter 4 brings a summary of the acquired results, conclusion obtained and limitations of this master thesis work . Additionally, suggestions are proposed to further improve the algorithm implemented in this work.

# 1 Introduction

## 1.1. The Respiratory System Anatomy

The main role of the respiratory system is the gas exchange with the external environment through the pulmonary airways in order to supply body with oxygen and remove carbon dioxide[1][2].

The respiratory system, functionally, can be separated in two zones:

1) **Conductive zone** (upper and lower airways). Its role is the conduction of air from the environment toward the site of gas exchange. It includes nose, pharynx, larynx, trachea, bronchi, and lungs[61]. This zone filters, warms and humidifies the incoming air. Further functions are coughing, voice production and swallowing (Fig. 1.1).
2) **Respiratory zone**. It represents the site where gas exchange occurs. It includes bronchioles, alveolar ducts and alveoli[61].

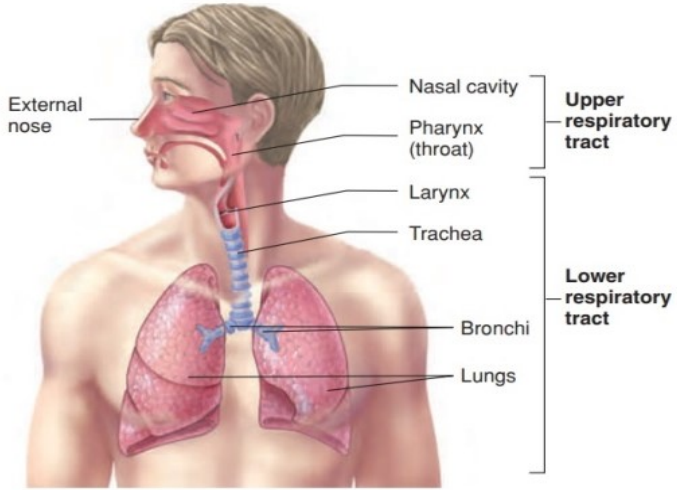


Figure 1.1 Anatomy of the respiratory system[a]

### 1.1.1. Conductive Zone

***Upper airways:***

Nose and nasal cavity. It provides an opening for the entering air. It has several functions including the filtering of air from external particles and the trigger of sneezes when stimulated by irritating particles, moreover it behaves as a resonating chamber for the acoustic waves generated by vocal cords[62].

Pharynx. It is a tube that connects the posterior nasal and oral cavities to the larynx and the oesophagus. It is divided into 3 regions: nasopharynx, oropharynx and laryngopharynx.

***Lower airways:***

Larynx. It starts just below the laryngopharynx and extends till the trachea. It is composed by 3 main parts [63]:

• Epiglottis in the upper part, behaving like a valve which opens during breathing and closes during swallowing.

• A cartilaginous chamber in the intermediate part, where the vocal cords are located.

• Ligament in the lower part, connecting the larynx to the trachea.

The main functions of the larynx are [63]:

- Providing an air passage.
- Separating air and food into the proper channels. Larynx is a common entrance for both air and food, therefore a switching mechanism is present here to route the air in the trachea and the food into the oesophagus.
- Contributing to voice production, by hosting the vocal cords.

- Sphinctering functions, by closing during coughing, sneezing and Valsalva manoeuvre.

***Tracheo-Bronchial Tree:***

The air, entering the pharynx through the nose, is conducted to the lungs through the trachea.

The Trachea is a tube devoted to air transportation, its wall is surrounded by cartilaginous rings of U-shape which provide both mechanical support, granting the trachea to stay open during breathing despite pressure changes, and flexibility, giving the possibility of bending. The trachea wall is composed by three main layers which provide the function of filtering, warming up at body temperature and humidifying the air[1]:

- The Inner layer, a mucous membrane made by pseudostratified epithelium with cilia, whose role is to remove the mucus, containing impurities as dust particles, out of the lungs.
- The Intermediate layer, called submucosa
- The External layer, the adventitia, which is the connective tissue containing the tracheal cartilage, responsible for the function of support and bending.

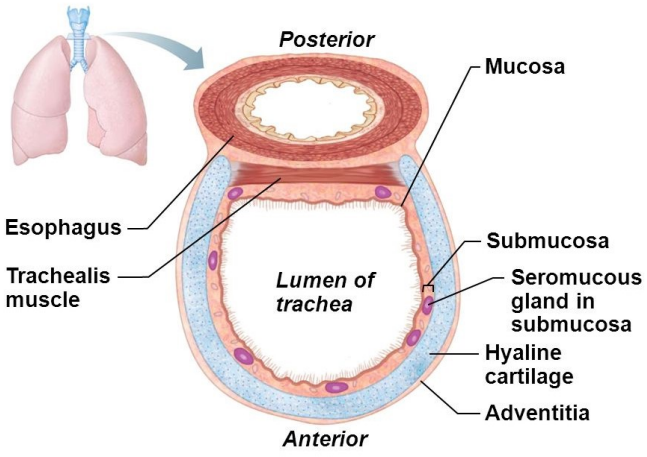


Figure 1.2 illustration of the layers that compose the cartilaginous ring visible by sectioning the trachea [e]

The trachea at the level of the carina divides into two main branches, the left and right bronchi, which enter the right and left lungs respectively.

Through the bronchi, the air enters a system made up by several ramifications, where the airways are organized as a branching network of tubes, with approximately 23 generations from the trachea to the alveoli, that become narrower, shorter, and more numerous as they penetrate deeper into the lung[3].

Bronchi entering the lungs start to split into secondary (or lobar) bronchi, each one supplying a sub-section of the lungs, called lobe. The right lung has three lobes, the lower, the middle and the upper, whereas the left lung has only two lobes, lower and upper.

Lobar bronchi, in turn, split into tertiary (or segmental) bronchi, each one supplying a sub-portion of the lobe, called segment. The right upper lobe has three segments (posterior, anterior, apical); the right middle has two segments (lateral, medial), the right inferior has five segments (superior, anterior basal, lateral basal, posterior basal, medial basal). In the left upper lobe two compartments can be identified: the superior and inferior, which contain three segments (posterior, anterior and apical) and two segments (inferior and superior), respectively. The left lower lobe includes five segments (superior or apical, lateral and medial basal and anterior and posterior basal).

The gross anatomy of the lungs and of the trachea-bronchial tree is depicted in Fig. 1.3.

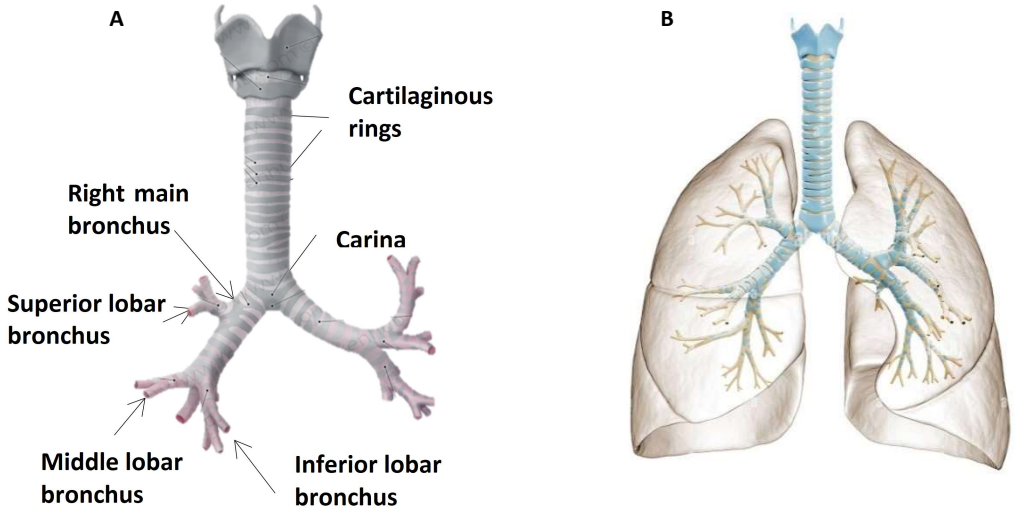


Figure 1.3 A) The trachea splits at the level of the carina into right and left main bronchus, which branch creating several ramifications; B) the right lung (on the left) which is subdivided into three lobes and the left lung (on the right) which is subdivided into two lobes, reached by the different airways generations[c][d].

Finally, each segment can be subdivided in lobules, which branch again to give rise to several orders of progressively smaller airways called bronchioles, the smallest of which are called terminal bronchioles[2].

The first ramifications are mainly devoted to the air transportation, while the terminal part of the Tracheo-Bronchial Tree corresponds to the respiratory zone which is devoted to gas exchange[2].

### 1.1.2. Respiratory Zone

It begins with the terminal bronchioles, which are the last components of the conducting portion of the respiratory system. Terminal bronchioles give rise to respiratory bronchioles, which ultimately lead to the alveoli (Fig. 1.4).

Alveoli are small sacs that, all together, provide a large surface for gas exchange. Inside there are pores connecting adjacent alveoli so that the alveolar pressure is equalized all over the lungs[1][d].

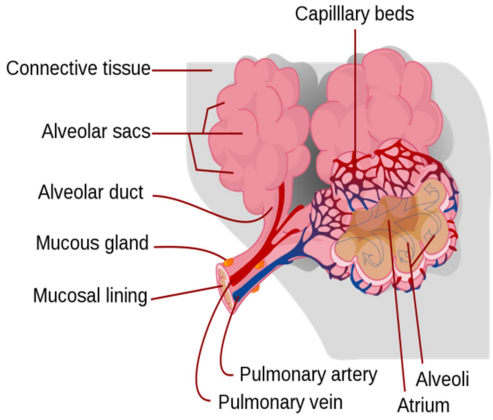


Figure 1.4 Anatomical structure of the components comprise the respiratory zone [f]

### 1.1.3. Geometry Of The Tracheo-Bronchial Tree

The human airways can be seen as a tree made by a lot of ramifications, where the root is the trachea, which represents the generation zero of the airway tree. At each branch division, called branchpoint or bifurcation point, an airway (parent branch) gives rise to two or more smaller airways (children branches), which form the new generation of the tree.

Going deeper and deeper in the bronchial tree, some structural changes occur[1]:

- The amount of cartilage decreases thus the airways becomes more flexible.
- Epithelium type changes, becoming less stratified and without cilia.
- The amount of smooth muscle increases: smooth muscles, typically, have the role to control the opening of the calibre of the airways, if they contract, the calibre is reduced.

Moreover, the number of ramifications increases, and the conducting tubes become smaller in diameter. The relevant dimension and characteristic of these ramifications are summarised in Figure 1.5.

| | GENERATION | NUMBER | MEAN DIAMETER (mm) | AREA SUPPLIED | CARTILAGE |
|---|---|---|---|---|---|
| Trachea | 0 | 1 | 18 | Both lungs | U-Shaped |
| Main bronchi | 1 | 2 | 12 | Individual lungs | |
| Lobar bronchi | 2 ↓ 3 | 4 ↓ 8 | 8 ↓ 5 | Lobes | Irregular shaped |
| Segmental bronchi | 4 | 16 | 4 | Segments | |
| Small bronchi | 5 ↓ 11 | 32 ↓ 2000 | 3 ↓ 1 | Secondary lobules | |
| Bronchioles Terminal bronchioles | 12 ↓ 14 | 4000 ↓ 16000 | 1 ↓ 0.7 | Pulmonary acinus | Absent |
| Respiratory bronchioles | 15 ↓ 18 | 32000 ↓ 260000 | 0.4 | | |
| Alveolar ducts | 19 ↓ 22 | 520000 ↓ 4000000 | 0.3 | | |
| Alveoli | 23 | 8000000 | 0.2 | | |

Figure 1.5 Dimension and structural characteristics of the Tracheo-Bronchial Tree [g]

## 1.2. Pathologies Of The Respiratory System

The pathologies affecting the Respiratory System are diseases which involve either the airways, the lungs, or the pleura, and can be grouped into two big patterns of dysfunctions[h] :

• **Obstructive:** comprises diseases characterized by a reduction in airflow, particularly during expiration, due to the obstruction of the airways. Examples of obstructive diseases are asthma, COPD, emphysema and bronchiectasis.

• **Restrictive**: comprises diseases characterized by an increase in lung stiffness and, consequently, a reduction of lungs size. Lung tissue becomes so rigid that is very hard to be expanded. Examples of obstructive diseases are pulmonary fibrosis and pleural fibrosis.

Respiratory system's diseases are very common medical conditions worldwide, and among them, asthma is one of the most diffuse diseases affecting the airways is Asthma.

### 1.2.1. Asthma

Asthma is a purely obstructive disease, correlated with an airway hyper-responsiveness. It is defined as a chronic inflammatory disorder of the airways that can range from mild respiratory compromise to life-threatening airway closure. The symptoms include recurrent episodes of wheezing, which is more common during the expiration because the airways normally narrow during this phase of respiration, breathlessness, chest tightness, and coughing, that can vary over time and in intensity[5][6].

As with many chronic conditions, asthma develops differently in each person. In particular, asthma can be classified according to its degree of severity. The severity is

determined by the frequency and intensity of symptoms and is assessed through lung function tests, such as spirometry and +peak flow test. It is important to understand the type of asthma affecting a patient, to keep it under control and provide the most accurate treatment [o][p].

The first distinction is between *intermittent* asthma and *persistent* asthma.

- Intermittent Asthma. The symptoms of wheezing and coughing happen no more than two days a week, night time flare-ups occur, at most, twice a month and outside of these few episodes the patient is free of asthma symptoms. So, intermittent asthma do not interfere with daily activities and breathing tests are within normal range[o][p].

If these symptoms worsen, the persistent asthma is considered with its three levels of severity [o][p]:

- Mild Persistent Asthma. The symptoms occur more than twice a week but less than once a day, and flare-ups may affect activity. Night time flare-ups occur more often than twice a month but less than once a week. So, it has still a little impact on daily life and physical activity. It can often be controlled by using a rescue inhaler, and breathing tests remain within the normal range.
- Moderate Persistent Asthma. Symptoms occur daily. Flare-ups occur and usually last several days, coughing and wheezing may compromise normal activities and make it difficult to sleep. Night time flare-ups may occur more than once a week. Moderate persistent asthma causes limitations on daily physical activity and lung function is approximately between 60% and 80% of normal, without treatment.
- Severe Persistent Asthma. Symptoms occur daily and often. They provoke an extreme limitation of daily activities due to the frequent asthma attacks, and a rescue inhaler is needed several times a day, every day. Breathing tests present low scores and lung function is less than 60% of the normal level,

without treatment. Severe is the least-common asthma level. Wheezing is no more present only during expiration but also during the inspiration phase, which suggests more severe airway narrowing.

Airflow limitation is a defining feature of asthma and it is suggested that in mild and moderate asthma the airway narrowing is reversible while in severe asthma airway obstruction may become permanent and less responsive to treatment[24].

All the structures of the airways are involved in the inflammation process of asthma[7][8][9]:

- Epithelium increases due to the hyper secretion of mucus and liquid, caused by the inflammation.
- Basement membrane increases in thickness due to collagen deposition.
- Airway wall changes in composition, content and organisation of the cellular constituents. In particular, there is an increase in the number of inflammatory cells, like eosinophils, mast cells and macrophages, (involved in the bronchoconstriction and mucous secretion process), and fibroblasts (responsible for the production of collagen);
- Smooth muscle, show hypertrophy (increase in the size of airway smooth muscle cells) and hyperplasia (increase in the number of airway smooth muscle cells). This leads to smooth muscle contraction, that contributes to the reduction of the airways calibre and to the increase in the airflow resistance.
- Mucous glands induce an hyper-production of mucus. They are distributed throughout the airways and are even present in peripheral bronchioles where normally they are absent. Their volume in the segmental bronchi of asthmatic patients is considerably larger than in normal subjects.

These morphological changes induce an alteration of the airway structure, called *airway remodelling*, that consists of a thickening of the bronchial wall, which leads to the narrowing of the airway lumen and to airflow obstruction. Airways remodelling can be reversible or irreversible and affects all the parts of the tracheobronchial tree, starting from the small airway and then progressing to the large airway[10].

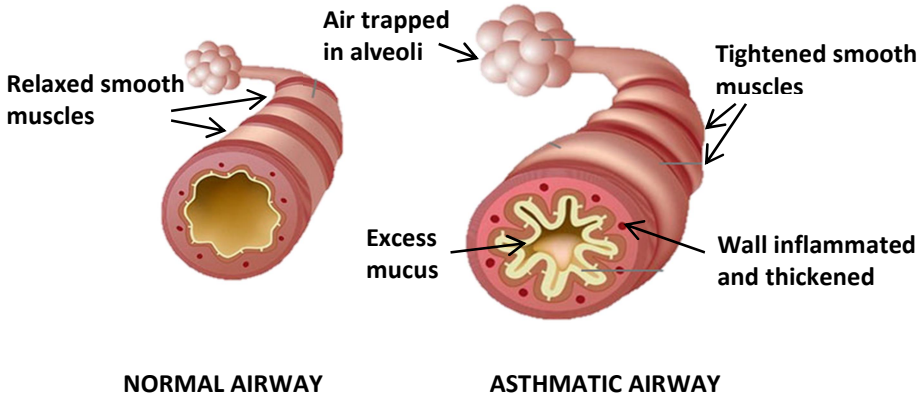


Figure 1.6 Airway Remodelling: the structural changes of airway in patient affected by asthma compared with normal airway[i]

## 1.2.2. Diagnosis

Investigations about airway remodelling are necessary to assess changes over time and elaborate new therapeutic interventions designed to attenuate or reverse these structural changes[52].

Pulmonary function test (PFT) are the first test to measure the global expiratory airflow limitation.

### 1.2.2.1. Pulmonary Function Test

Pulmonary function tests (PFTs) are non-invasive tests that assess global lung function

Spirometry is the most common of the PFTs which measures the ability to inhale and exhale air relative to time. It is executed through the following procedures:

1) Maximal inspiration: the patient is asked to take a full inspiration;
2) A "blast" of exhalation: the patient is asked to perform a complete forced and full expiration, till lungs are completely empty.

The main results of spirometry are:

- Forced Vital Capacity (FVC): it is the difference between the maximum volume of air inspired with a full inspiration and the minimum volume of air remaining in the lungs at the end of a forced expiration; FVC quantifies the maximal expansion of the lungs, so the maximal breath that a subject can take.
- Forced Expiratory Volume exhaled in the first second (FEV1): it is the volume expired by a subject in 1 sec, after the starting of the forced expiration.
- FEV1/FVC ratio, called also Tiffeneau index: in normal conditions it is around 80%, meaning that in the 1st second a subject typically expires the 80% of the whole air contained in the full lungs.
- Parameters related on the pulmonary flow as Forced Expiratory Flow (FEF) and the Peak Expiratory Flow (PEF).

In principle, spirometry is based on a simple manoeuvre, but it can be difficult for patients with severe respiratory disease. Thus, the test is repeated 3 times.

All these parameters change in presence of obstructive and restrictive diseases. In normal healthy subjects the FVC is equal to 5L and FEV1 is the 80% so 4L.
In obstructive diseases the expiratory flow is limited, the expiration is prolonged and requires more time to be completed, so FEV1 is reduced, as well as FEV1/FVC.
In restrictive diseases, lung tissue becomes rigid and its maximum expansion decreases, thus FVC decreases and FEV1/FVC increases[25] .

These parameters can be obtained easily and are rich of clinical information about lung function, but they represent global measures and do not identify the precise location and the extent of airway abnormalities represented by the airways remodelling[11].

#### 1.2.2.2. Bronchial Biopsy

Originally airway remodelling in asthma has been studied in vivo by performing bronchial biopsies. Bronchial biopsy specimens have been used in asthma research since late 1970s because can provide valuable information about the inflammatory and morphological changes on the various anatomical structure of airways, such as epithelium, basement membrane, submucosa, and smooth muscle, that is why they represent a useful tool to study airway remodelling in asthma. Bronchial biopsies can be obtained via bronchoscopy, during which a thin tube, the bronchoscope, is passed through the nose or mouth down your into the lungs, at maximum to the segmental airways, from which biopsy of tissue is performed [26],[27],[q].

Bronchial biopsy represents a useful tool to study airway remodelling in asthma, but it is limited both by the invasive nature of the procedure, as require access to surgical or autopsy samples of the airways[12] , and by the inability to sample all the components of the bronchial wall and the small airway more distal [27].

In this sense computed tomography (CT) imaging offers new possibilities in the qualitative and quantitative evaluation of airways morphology in a non-invasive way, and it can be used to help diagnose and monitor the progression of the disease[53].

## 1.3. Computed Tomography Imaging

Computed Tomography, or CT, refers to a computerized X-ray imaging procedure that allows to obtain thin cross-sectional images or 'slices' of patient's body, and, once enough adjacent slices are collected, they are digitally "stacked" together to form a three-dimensional (3D) image of the patient that allows for an easier identification of basic structures as well as possible diseases or abnormalities. Moreover, in addition to transverse slices, coronal, sagittal, and other (oblique) slice planes can be reconstructed from the 3D volume data[1] (Fig.1.7).

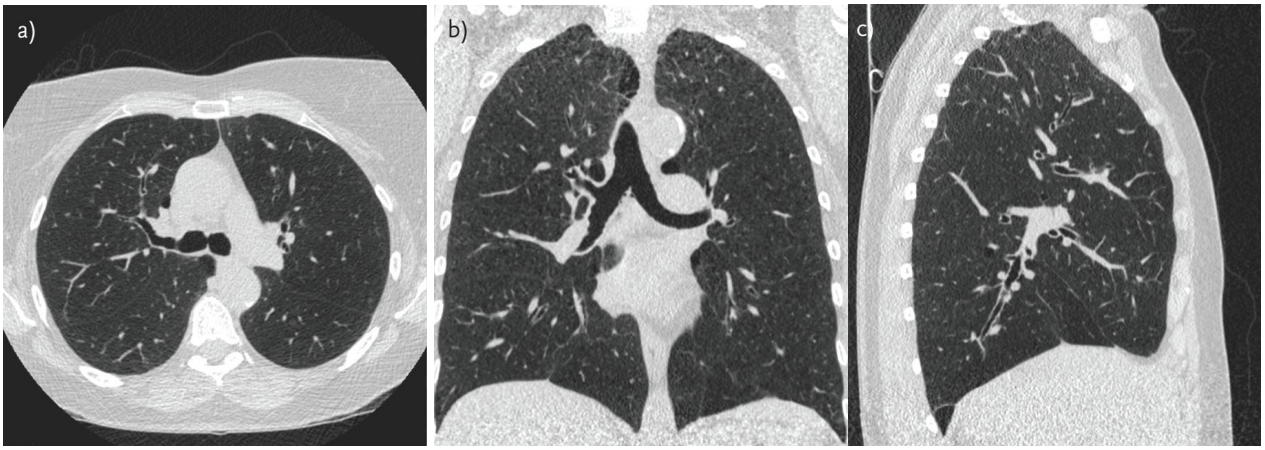


Figure 1.7 CT scan acquired using a multi-detector row CT scanner. a) Conventional transverse image b) coronal and c) sagittal reformats of the CT data of normal lungs[13] .

The CT scanning unit, the gantry, is the structure containing the X-ray tube and the photon detectors which are positioned to face each other and are built to rotate 360 degrees around the patient. In the last generation of CT scanner many more stationary detectors are introduced arranged in multiple rows (called multi-row detectors) providing the scanning of multiple tissue slices simultaneously, reducing scan time, granting an higher resolution and improving efficiency in the use of X-ray tube power.

The X-ray source produces X-rays beams which irradiate a body section, and the attenuated X-rays exiting the body are acquired by the detectors. The collected data are stored to a computer where they will be reconstructed into cross sections images of the body [m].

The X-ray attenuation, or photon absorption, differs according to the density of the anatomical structure crossed by the beam. The CT detectors measure this amount of attenuation and converts it in such a way to assign a proportional value of brightness to the displayed pixels in the resulting image[14].

The result is a grey scale image, in which the information about the tissue density is encoded in the grey level value of the image pixels (Fig 1.8).

The scale's range of values is referred to the Hounsfield Unit (HU) scale, which is calculated considering a linear transformation of the baseline linear attenuation coefficient of the X ray beam, where 0HU is the value arbitrarily associated to water, -1000HU is the value associated to the air. For what concern the lungs, they can be considered as sponges of air and tissue, so with HU values ranging from -650 to -950. The airways can be seen as tubular structure made by soft tissue containing air, so they are visible on CT as a black portion (-1000HU of air) surrounded by a whiter structure (Fig. 1.8).

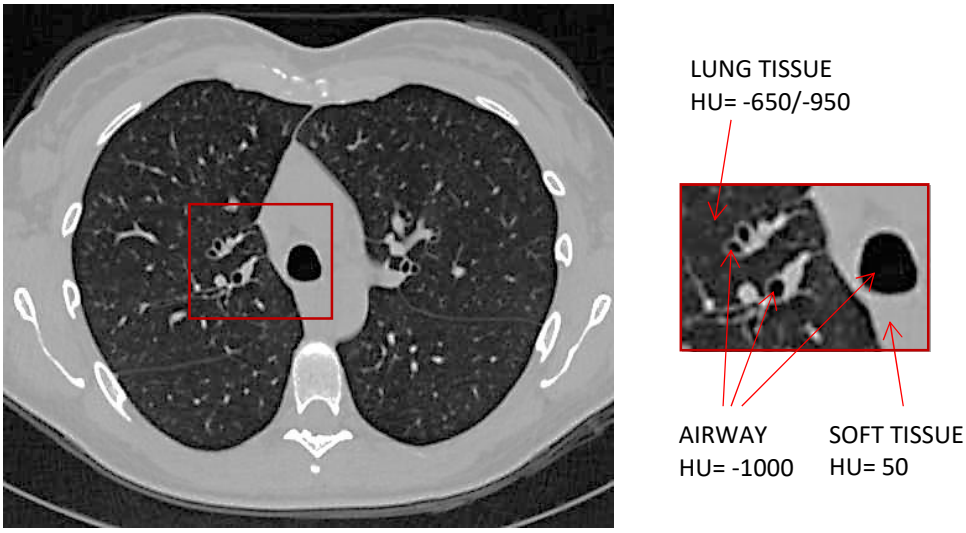


Figure 1.8 CT appearance of normal lungs and relative HU values

High-resolution CT is typically performed at full inspiration, when the maximal lung expansion and airways dilation are achieved .

On the contrary, CT images obtained at maximum expiration, are considered complementary studies to the inspiratory CT images. During expiration, a normal lung tissue increases homogeneously in CT attenuation, the lungs become smaller and there is an airways narrowing. Considering the trachea, its shape changes from round during inspiration to a letter-D during expiration, as illustrated in Fig.1.9. Typically, expiratory CT images are used to evaluate the air trapping, which is common in obstructive disease like asthma and is not visible in inspiratory CT images.

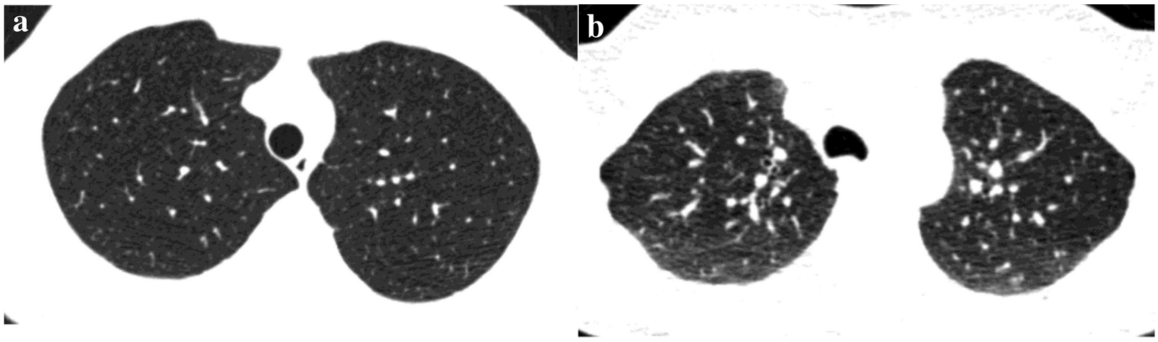


Figure 1.9 a) Inspiratory axial CT scan show the normal round shape of the trachea; b) expiratory axial CT scan shows the normal bowing of trachea, it is visible also the normal homogeneous attenuation increase of the lung tissue[28].

Changes in lung density on CT images are suggestive of pulmonary disease.

Failure of the lung tissue to homogeneously increase in attenuation during expiration indicates air trapping and suggests small airways disease like asthma. Typically expiratory CT images are used to evaluate the air trapping, which may be the only evidence of abnormality, as the lungs may appear entirely normal or near normal on inspiration [28] [34] .

### 1.3.1. CT Images in Asthma

In the following section, the main pulmonary alterations, that be visualized on CT in asthma, are described.

- Bronchial wall thickness. Abnormal thickening of bronchial walls can arise from a vast number of pathological entities[n]. It is a common feature in asthmatic patients, as results from the inflammation process of the airways and has been shown that the degree of thickening correlates with asthma severity and disease duration[15] .

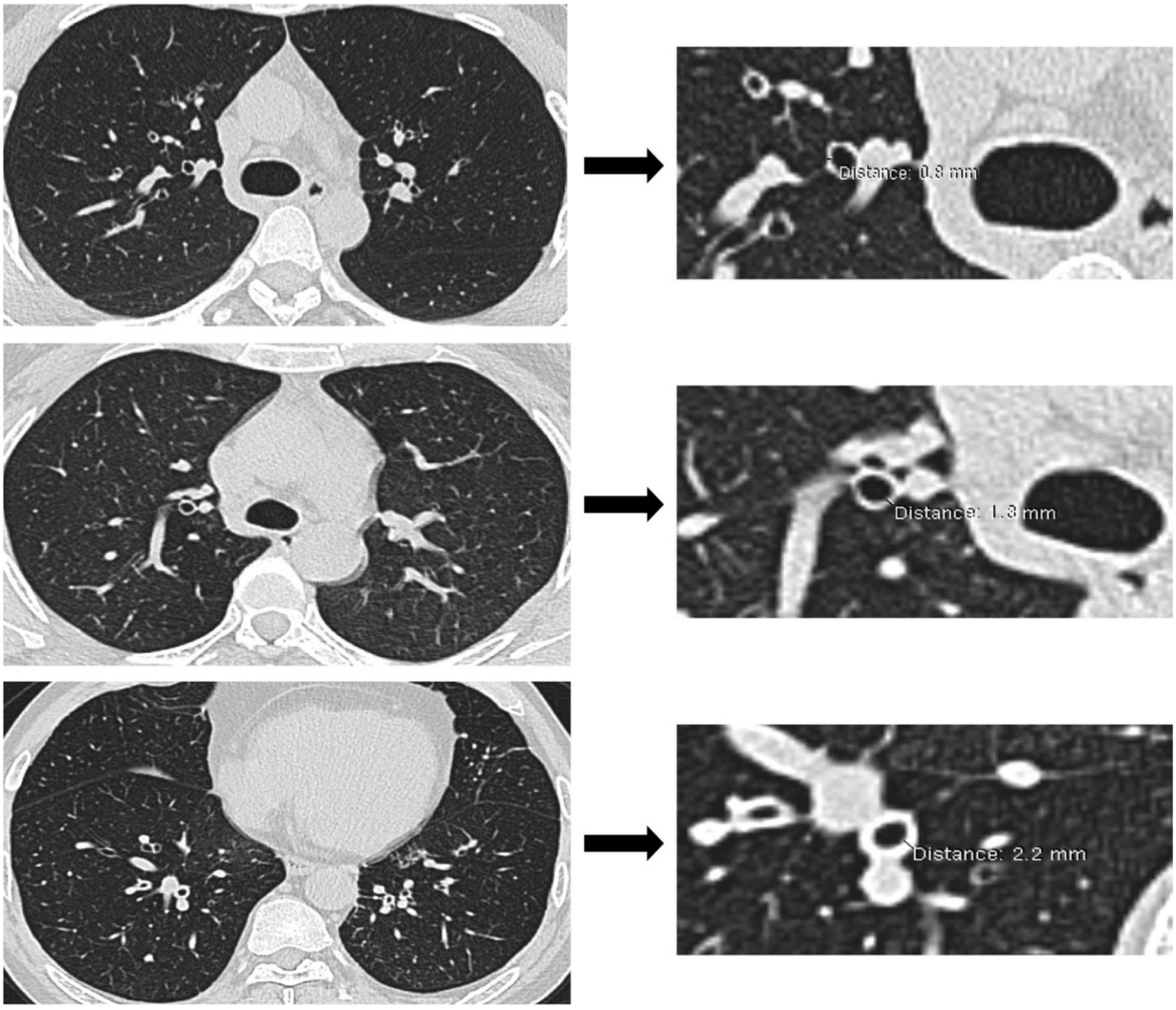


Figure 1.10 (A) normal bronchial wall (0.8 mm) from a patient with a one-year history of asthma; (B) mild bronchial wall thickening (1.3 mm) retrieved from a patient with asthma for one year; (C) moderate bronchial wall thickening (2.2 mm) in a patient with asthma for 19 years.[16]

- Mosaic lung attenuation. It describes a patchwork of regions of different pulmonary attenuation. In asthma the presence of this pattern is caused by the Air Trapping[n].

Air trapping refers to the retention of gas in the lung during expiration, due to a complete or partial airway obstruction, which prevents air to be fully exhaled. Air trapping can be identified on CT as an abnormal decreased attenuation of pulmonary parenchyma, [n], as shown in fig. 1.11.

Air trapping can be used to indirectly assess changes at the level of the smaller airways (peripheral membranous bronchioles <2mm in diameter), which are beyond the currently available resolution[15].


Figure 1.11 Air trapping in CT images of asthmatic subjects, the red arrows indicated darker regions within the lungs that indeed represent the air trapping[16]

Therefore, quantitative lung densitometry on CT can be used to study airway remodelling in asthma, by measuring the percent volume of air trapping, i.e. the percentage of lung parenchyma that is less dense than normally aerated lung tissue.

## 1.4. Quantitative Techniques For Airway Analysis

To evaluate disease progression or the effect of pharmacological treatments, quantitative information about the geometry of the airways should be extracted.

In initial studies, airway dimensions were measured relying on manual tracing of the airways in CT images. These techniques are extremely time consuming and prone to errors. Hence, automated and semi-automated algorithms for the computerized analysis of human airways have been developed and there is still research on it [12].

The common steps involved in airway analysis using CT images are as follows:

- Segmentation of the airways;
- Centerline extraction, also called skeletonization;
- Airways Morphometry Analysis.

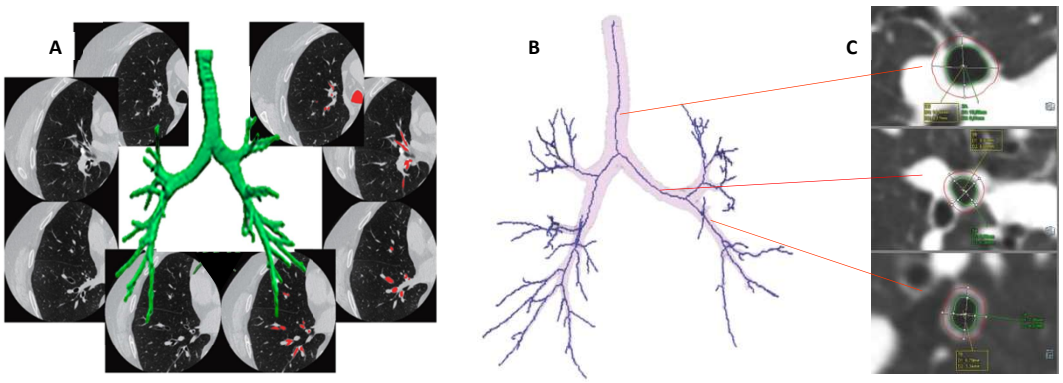


Figure 1.12 Flowchart for airway analysis: A) airway tree segmentation from the original 3D CT images; B) extraction of the centreline; C) through which extract interest airway parameters in different points[20][19] .

### 1.4.1. Segmentation

Many algorithms have been designed for the automated identification of the human airway tree. However, because of the relatively high contrast between the airway

lumen and the airway wall, a straightforward way for extracting the airway tree is to use a three-dimensional (3D) region-growing algorithm.

- Region-growing is a segmentation approach which starts by selecting an initial voxel on the image, called seed, which can be either traced manually by an operator or automatically detect and, for sure, belongs to the region to be segmented, that in this context is the airways lumen.

Then, the algorithm examines the neighbouring voxels of the seed and determines whether they should be added or not to the region according to some inclusion criteria that depends on a specified value of intensity threshold. Voxels of similar intensity and connected to the initial seed point are marked as belonging to the region. Region-growing is a very simple and efficient procedure, thus many segmentation methods are based on this approach, while others use it as an initial step implementing additional procedures to avoid leakage[17][22] .

According to the employed methodology, segmentations algorithm can be classified as[17][18]:

- Morphological based methods. The identification of the airway tree is based on two steps: 1) detect two-dimensional circular structures and 2) reconstruct the 3D airway tree starting from the detected circular structures. This method aims to explore the shape, size, and intensity specific for the airways, and also their spatial relationship with the adjacent slices[38][17] .
- Knowledge or rule based methods. The anatomical knowledge about airways and blood vessels are used to perform airway identification. Candidate airways are recognized on individual slices based on some known proprieties, as the adjacency to the vessels, the expected dimension, the progressive decrease in diameter, the

expected region grey level, and the absence of abrupt changes in branching angle[39][17] .

- Template matching based methods. In order to detect the airways on CT images, a set of 2D/3D predefined templates are used with a shape comparable to the one of the airways. For this reason the most suitable and used template is the 2D circular template. But airway appears circular just in the perpendicular direction of the scanning plane, so also a 3D cylindrical template is exploited to overcome this limitation [41][17].

- Machine learning classifiers-based methods. Identify candidate airways considering the underlying probability distribution of specific airway characteristics by automatically summing up the potential patterns, distinguish the actual airways from non-airways [40][17].

### 1.4.2. Skeletonization

It is referred to the medial axis extraction or thinning operation of the segmented trachea-bronchial tree. The extraction of the centreline is useful to guide the accurate detection of airway geometry, and it is also natural for the treelike structure of the airway [17][19].

### 1.4.3. Morphometry Analysis

It is the analysis of the airway morphology[17][19][20]. The algorithms for the extraction of airway morphological parameters perform the following steps, outlined in Fig. 1.13:

- Resample the two-dimensional slices orthogonal to the centreline to minimize errors due to the oblique orientations of the airway.
- For each two-dimensional slice separately, segment the lumen-wall and wall-lung parenchyma boundaries on the airway.
- Measurements of parameters of interest.

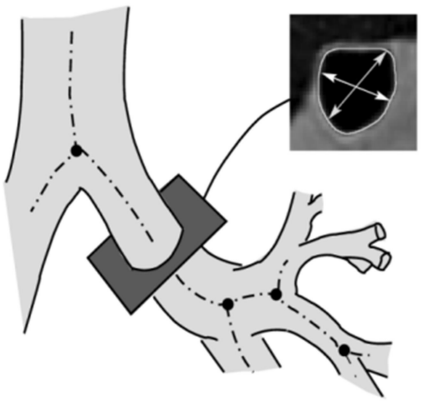

Figure 1.13 illustration of the steps for the morphometry analysis[20]

### 1.4.3.1.Parameters

The most relevant parameters concerning the dimension of the airways are reported in Figure 1.14 and are the followings[21]:

- The maximum and minimum diameter of the internal lumen (ID1, ID2), as the lumen can be not perfectly circular.
- Bronchial wall thickness (WT), that has been demonstrated to be larger in asthmatic patients than in healthy subjects.
- Lumen area (LA), Wall area (WA), Total area (TA): as the airway borders are irregular seen on CT images, it is preferable to use measures related on the areas of the airway than perimeters or distances. Moreover, as airway size

may be affected by body size, WA and Ai are are normalized by the body surface area (WA/BSA, Ai/BSA).)

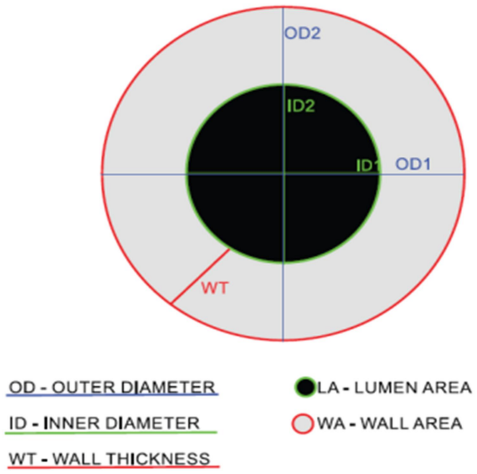


Figure 1.14 illustration of the bronchial tree main parameters[24] .

However, these measurements can vary widely even within the same airway segment and so a high number of them should be calculated for each airway segment in each patient. Due to this fact other measurements have been considered which are more representative of the same patient and less dependent from the high variability of airway's size among different patients, like:

- WA%: wall area normalised on total area, WA% = (WA/TA) × 100.
- Pi10: the value of the square root of the area of the airway wall having an internal perimeter of 10mm.

Among these parameters, the calculation of the lumen area and the internal diameters results to be trivial, as can be directly assessed from the segmentation algorithms mentioned above and designed for the airways lumen identification.

Conversely, for the bronchial wall thickness some additional efforts are needed to detect the outer airway wall[17].

### 1.4.3.2. Algorithms For Parameters Measurements

Accurate measurement of airway wall dimensions has remained a challenge mainly due to the difficult identification of the outer wall which is often compromised by surrounding parenchyma and vessels. Several attempts to accurately measure airway structures can be found in literature, but the two most applied techniques are the *Full Width at Half Maximum (FWHM)* and *Phase Congruency*.

FWHM method:

To estimate the inner and outer wall locations, a certain number of rays is projected from the centre of the airway lumen outward to the parenchyma and the intensity profile along each ray is measured. According to the FWHM principle, the outer and inner airway wall are assumed to be located halfway between the local minimum value within the lumen and the maximum value within the wall, that is the FWHM location, as shown in Figure 1.15. This is the most simple method for the estimation of the airway wall thickness.. However, the measurement can be biased due to partial volume effect and CT reconstruction algorithm, moreover, there might be leakages of the airways into the lung parenchyma due to the presence of adjacent vessels.[17]

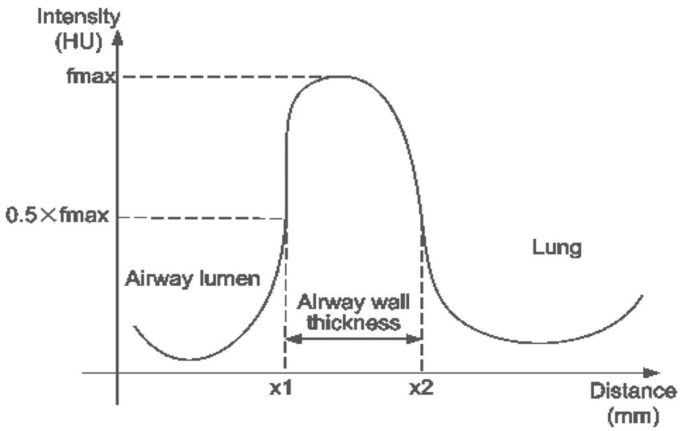


Figure 1.15 illustration of the FWHM method for the airway wall identification, the curve denotes the intensity profile of a ray [17] .

Phase Congruency method :

The method is based on the phase congruency principle according to which relevant features, as edges or lines, can be detected where the local phase exhibits maximal coherency. Phase congruency is an intrinsic property of a signal that is preserved even when the signal undergoes smoothing, as the one introduced by the point spread function (PSF) of the scanner [22][17].

One approach to measure it is by providing different approximations of the signal, using different PSFs to generate the final CT images. The overall behaviour of the PSF can be modified by choosing different reconstruction kernels. A reconstruction kernel is a parameter of the reconstruction process and specify how the neighbouring samples in the projection space are averaged before the back-projection to compute the final intensity value of each pixel[22]. Figure 1.16 shows the effect of phase congruency on an airway reconstructed with nine different kernels.

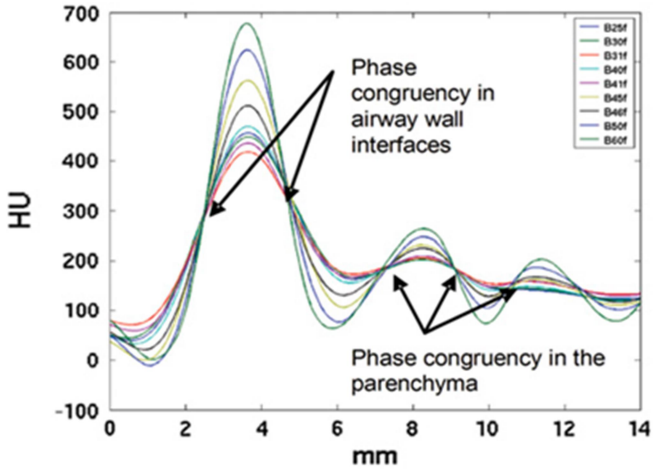


Figure 1.16 Airway wall localization by means of phase congruency using multiple kernels [22].

The location where the intensity profiles from different kernels intersect in common crossing points is an indicator of maximal phase congruency and can be used as an estimator for airway wall location [17][22].

This method is shown to be robust, accurate and reliable in providing measurement but it is computationally intensive[22].

## 1.5. Literary Review

Algorithms for quantitative analysis of airways morphology and their structural changes due to respiratory diseases have been widely explored in literature. These studies differ in the number of airways considered, in the number of measurements calculated or in the algorithm used, but they always reached similar conclusions, in particular a reduction of lumen area and an increase in bronchial wall thickness is present in asthmatic with respect to healthy subjects, especially in more distal airway[24].

### 1.5.1. Comparison Between Asthmatic And Healthy Subject

Patyk et al.[24], aim to both evaluate the usefulness of quantitative multi-slice computed tomography in the assessment of airway wall thickness and to verify the relationship between the structural changes of bronchial tree and the airflow limitation in patient with asthma. This study was performed considering a group of patients with well-defined long-term asthma and a control group composed by healthy volunteers. All the examined subjects undergo to a CT scan at full inspiration and wall thickness, lumen area and inner diameter were measured from the third up to the ninth generation of the posterior basal bronchi of the right lung. Lung function

tests, as spirometry, were also performed the same day as the CT scans to retrieve the measured forced expiratory volume in 1s (FEV1), forced vital capacity (FVC), peak expiratory flow (PEF) and respiratory resistance (Rocc). The study demonstrated an increase in airway wall thickness in asthma patients compared to healthy volunteers, particularly in the medium and small airways (fifth to the ninth generation of the bronchi).

Moreover, a significant relationship between the quantitative CT parameters and Lung Function Test parameters, mainly FEV1, was found.

### 1.5.2. Comparison Among Subjects With Different Asthma Severity

Other studies were more focused in finding a correlation between the airways structural changes and the severity of asthma.

Niimi et al.[29], in a group of patients having different degree of asthma severity, measured the lumen area (LA) and total area (TA) in five points of each airway in the apical bronchus of the right upper lobe. This site was chosen because of its more convenient orientation for obtaining a tangential view, as well as an outer perimeter view of the airway not abutted by vessels or other bronchi. From these measurements the parameters of wall area (WA), wall area corrected by body surface (WA/BSA) and wall area percentage (WA%) were calculated. Both WA and WA/BSA were significantly correlated with asthma severity and with the duration, supporting the hypothesis that there is a progressive increase in airway wall thickening with increasing duration as well as severity of asthma. Furthermore, a significant negative correlation was found between WA or WA/BSA and the indices of airflow obstruction FEV1 or FEV1/FVC, and not such strong correlation was found between WA% and clinical indices of asthma, supporting the hypothesis that WA is a more appropriate measure of airway wall thickness than WA%.

The authors found also that LA or LA/BSA did not decrease, as they expected, with the increasing of severity of asthma and explained this phenomenon by the presence of the bronchial dilatation or bronchiestasis effects reported in many descriptive CT studies of airway abnormalities in patient with severe asthma. These effects are more present in patients with more severe asthma and involve the increase in the airway lumen area. Another possible explanation regards the increase of lung volume with increasing of asthma severity, accordingly airway diameter, or luminal area, becomes larger.

Similarly, Hoshino and colleagues[30], assessed the relationship between airflow limitation and airway dimensions from the third to the fifth generation of bronchi, considering subjects with different degree of asthma severity.

CT images were analysed using automated software designed to segment the first five airway generations and to measure lumen area and total area using the FWHM principle. In this study two bronchi were selected, the apical bronchus and the posterior basal bronchus of the right lung, and the measurements were calculated at three different points of each segment.

It has been reported that patients with severe asthma had a greater airway wall thickness and, conversely from the Niimi et al.[29] report, also smaller lumen area than those with mild asthma. These observations were particular evident at the fifth generation, where airway wall thickening, measured as WA%, was greater and airway narrowing, measured as Ai/BSA, was smaller in severe asthma compared with those of mild-to- moderate asthma. Moreover, the correlation between airways wall dimension and airflow limitation was higher in correspondence of distal airways, so they concluded that remodelling in asthma occurs dominant in the more distal airways than large airways. Differently from Niimi and colleagues, a poor correlation between CT measurements and disease duration was found while a

significant correlation between WA% and FEV1% was determined, in particular at generations 4 and 5.

This study concludes that quantitative analysis of airway dimensions using non-invasive MDCT identifies distal airway changes and would be useful to evaluate the efficacy of airways treatment and diagnosis.

### 1.5.3. Relation Between Airway Remodelling Assessed By CT and Functional Data

Many studies evaluate the airway structural changes, evaluated by CT, in patient with asthma and correlate these morphologic abnormalities with clinical features, in particular pulmonary function test and also biopsy specimens.

Kasahara et al.[31], aim to find a correlation between the bronchial wall thickening, and the bronchial epithelial reticular basement membrane (Rbm), obtained by biopsy examination, which contributes to airflow obstruction, airway hyper-responsiveness, and respiratory symptoms. In addition, they examined the association of both Rbm and whole wall thickening with airflow obstruction. The relevant morphological parameters (WA% and WT%) have been extracted from CT at five levels: the superior margin of the aortic arch, the tracheal carina, 1 cm below the carina, the inferior pulmonary veins, and 2 cm above the diaphragm. Then five biopsy specimens were taken from subsegmental bronchial bifurcations in the right lower lung in each subject and the Rbm thickness is calculated as the ratio between the area of the whole Rbm and the length of basement membrane. Moreover, pulmonary function tests were performed through spirometry to measure the FEV1 and the peak expiratory flow.

The results showed that both WA% and WT% are significantly higher in patients with asthma than in healthy controls at all lung level, and that there is a strong

positive correlation between airway wall thickness and Rbm thickness. The Rbm thickness, WA% and WT% are significantly and negatively correlated with %FEV1, suggesting that thickening of the airway wall assessed either in biopsy specimens or by CT scanning is also correlated with airflow obstruction.

Similar studies were conducted with similar results. Berair et al.[32], described the relationship between qCT and endobronchial biopsy specimens and showed a significant correlation between bronchial cross-sectional lumen area and the epithelial thickness, especially in proximal airways. Tsurikisawa et al.[35], in addition, demonstrated a significant correlation between the duration of asthma and airway structural changes, showing that asthma duration was inversely correlated with FEV1%. Furthermore Cohen et al.[36], found the epithelium thickness on the biopsies was significantly greater in subjects with severe persistent asthma compared with those with mild persistent asthma, normal and diseased controls .

### 1.5.4. CT And Hyperpolarized Gas MRI

Computed tomography have been applied to assess structural changes caused by airway remodelling. Actually, during a CT acquisition, the patient absorbs a certain dose of radiation, so CT scanning cannot be repeated often to not expose the subject to the risks of excessive radiation.

In this sense the new frontier of the research is represented by the use of hyperpolarized gas MRI, where hyperpolarized noble gases, as Helium-3 or Xenon-39, have been used to investigate the regional patterns of airflow obstruction within the lung. Hyperpolarized gas MRI has an advantage over CT as no ionizing radiations are required, moreover, the rapid clearance of the gas from the lungs permits repeated evaluation of individual subjects[27][54].

Hyperpolarized gases are used as inhaled contrast agents to enhance the MR signal and so provide MR images of the lung airspaces with high spatial resolution. Introducing gas through the airway into the lungs allow to see which airway is actually participating in the ventilation of the lung[54]. For this reason, hyperpolarized gas MRI can be used to detect the persistent airflow obstruction in some areas of the lungs which is a distinctive characteristic of pathologies like asthma[27].

When the hyperpolarized gas is inhaled the airspaces are filled and when subsequently MR images are obtained, the changes in the regional ventilation resulting from airflow obstruction are detectable.

In healthy subjects, inhaled helium-3 distributes evenly throughout the airspaces of the lungs through the airways. When there is a focal reduction in airflow, the airspaces distal to the narrowed airways do not fill with the gas and appear dark on the images, defining the so-called ''ventilation defect'' (Fig. 1.17). Focal ventilation defects have been found in a variety of obstructive lung diseases, such as asthma[54].

Figure 1.17 hyperpolarized MR image with Helium-3 of asthmatic patient and ventilation defect (white arrows). The part of the image coloured in grey are the region of the lungs reached by the gas, the black portion of the lungs are the ones affected by the ventilation defect.

Holmes et al.[37], compared findings of CT with hyperpolarized helium-3 MRI findings during forced expiration. They recruited both asthmatic and healthy subjects. In CT images, the presence of focal regions of low attenuations were considered areas of air trapping, in MRI images the presence of a persistent signal with expiration were considered to be related to air trapping and, moreover, Holmes and colleagues found a general concordance between these areas of air trapping on the two imaging modalities[27].

Also Fain et al.[33], aimed to assess regional disease in asthma by comparing the locations of ventilation defects on Helium-3 with the locations of air trapping on MDCT. This comparison revealed a significant overlap between the two, suggesting that the locations of airway obstruction and air trapping are associated in asthma.

Aysola et al.[27], in their study reviewed the application of CT-based techniques and hyperpolarized gas MRI to study structural and functional changes in asthma and showed that asthma has a regional distribution within the lung, causing the fact that some areas of the lung are more affected than others. They come to the conclusion that a potent tool for directing asthma treatment may result from the possible combination of structural information from CT and functional information from hyperpolarized gas MRI.

# 2 Material and Methods

The objective of this thesis work is the extraction and accurate measurement of the relevant morphological parameters concerning the airways geometry on CT images. The procedure followed to achieve this goal is represented in the following block diagram (Fig. 2.1). The main steps are: implementation of the algorithm for airways segmentation and analysis, validation of the designed algorithm through the comparison of the automatically retrieved measurements and the manually extracted measurements, comparison between the data measured in healthy and asthmatic subjects.

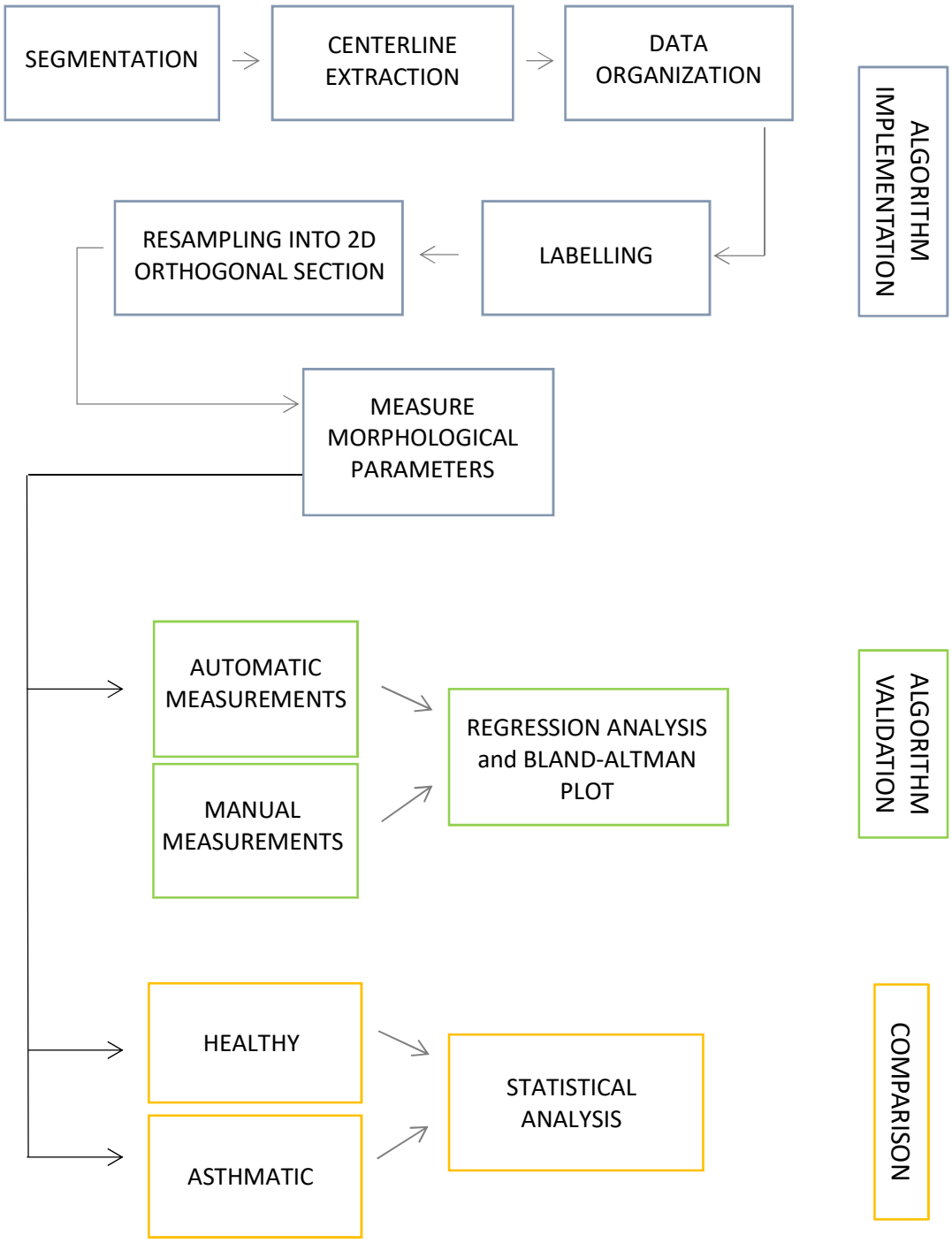


Figure 2.1 Block diagram representing the overall procedure implemented in this work

**DATASET:**

The population considered in this study is composed by five healthy subjects (controls) and five patients with asthma.

Each patient was scanned in supine position at maximum inspiration, near total lung capacity (TLC).

Imaging acquisition parameters are: matrix of 512x512 pixels, slice thickness equal to 1mm in healthy and 0.75 mm in asthma, pixel spacing included in a range from 0.5mm to 0.71mm.

## 2.1. Algorithm Implementation:

The main steps include:

1. Segmentation of airway lumen;
2. Centreline extraction;
3. Morphometry analysis .

### 2.1.1. Segmentation

The algorithm for segmentation was already available in C++ language, using the ITK library. In this work, the algorithm has been converted in Python language using the same ITK library[42][43].

This algorithm can be divided into two main functions:

1. Segmentation of the trachea;
2. Segmentation of all the other airways from the trachea.

2.1.1.1. Trachea Segmentation

Thresholding and Removing the Background:

The first step for trachea segmentation is the thresholding of the greyscale image into a binary image, by applying an optimal thresholding algorithm through an iterative process, which separates low-density tissue (i.e. lung, airways and air surrounding the patient) from the surrounding chest wall (i.e. mediastinum, and large blood vessels).

Finally, the background air is eliminated by deleting the regions connected to the border of the image, retaining only the lungs and the airways (Fig. 2.2).


Figure 2.2 A) original grayscale image; B) thresholded image; C) thresholded image without the background

Trachea Reconstruction:

The trachea is identified in the binary image by searching for round elements having the centroid in the central region of the image.

This function exploits the 'BinaryImageToShapeLabelMapFilter' class of ITK, which converts the binary image into a label map to evaluate the shape attributes which, in this application, are roundness and position.

The output is a 3D binary image depicting the internal lumen of the trachea only.

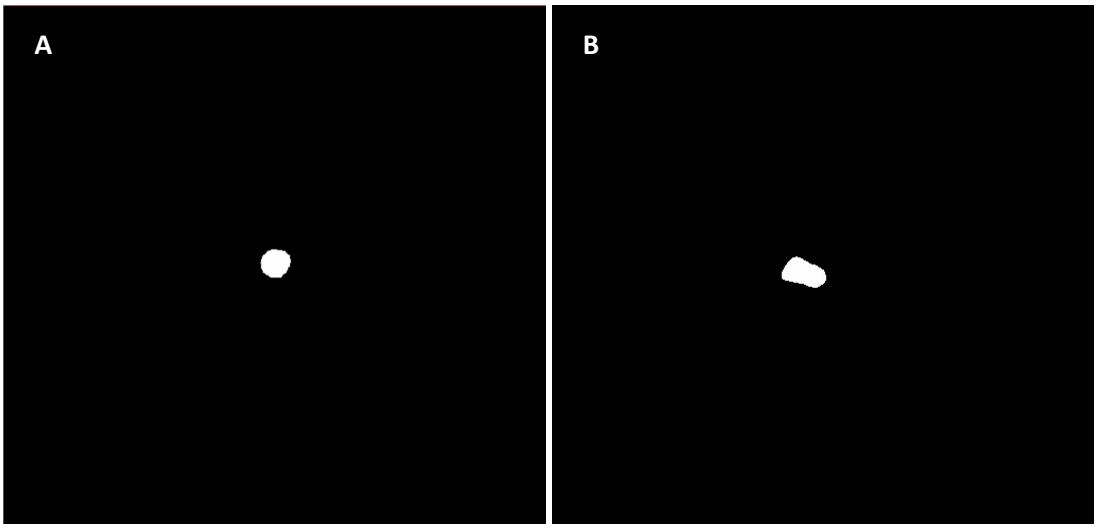


Figure 2.3 segmentation of the Trachea, it is noticeable that no other airways are present. The two images refer to the middle point (A) and to the carina (B) below which no other object is depicted.

#### 2.1.1.2. Bronchial-Tree Segmentation

The segmented trachea, the original grayscale image and the thresholded image without the background are the input of this step.

The original image is first filtered by the 'CurvatureFlowImageFilter', which that preserves the sharp boundaries, a smoothing only within region with similar intensity. Then, a region growing algorithm is applied. The region growing algorithm is implemented by using a 3D confidence connected region growing algorithm. The seed is the segmented trachea whose pixels have an intensity value lower than a given threshold, set to the mean intensity value of the trachea pixels.

The region growing is implemented within an iterative cycle and at each new iteration the previous reconstructed tree is given as seed.

The leakage of the tree into the lung parenchyma can represent a drawback of the region growing procedure for the bronchial-tree segmentation. In this algorithm it is avoided by retrieving the intensity value of the new pixels added as seeds and checking that it is lower than the mean value.


Figure 2.4 result of the segmentation of the Tracheo-Bronchial Tree: A) 3D view; B) transverse view at the carina level.

### 2.1.2. Centerline Extraction

The centreline can be easily extracted using the related function of the scikit-image package[44] available in Python, in which a thinning process is applied to the binary image of the segmented tree to reduce each connected component to a single-pixel wide skeleton. The centreline extraction, also called 'Skeletonization', facilitates the creation of the tree data structure and the orderly exploration of the trachea-bronchial tree explained in the following step.

Before retrieving the centreline, the segmented image is filtered with morphological operations, specifically a Closing followed by an Opening operation, to obtain a centreline as clear as possible without 'bubbles' effects and spurs (Fig. 2.5), (Fig. 2.6).

The Closing operation consists of a dilation followed by an erosion process and it allows to close small holes (black points) of the object. The Opening is the reverse operation, as it performs an erosion followed by dilation and it is used to remove noise.

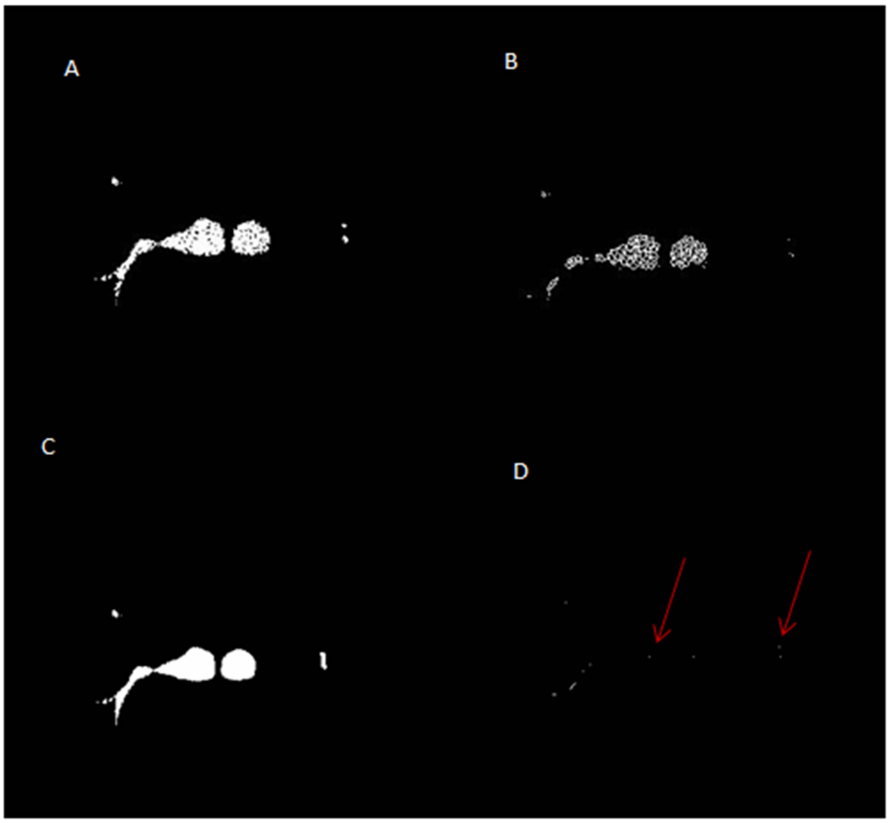


Figure 2.5 Some segmented images (A) may present holes inside, leading to an erroneous centerline (B) with a 'bubbles' effect; it can be fixed by applying a Closing filter (C) on the segmented image which leads to obtain white pixels (red arrows) just in correspondence of the skeleton of the airways (D).

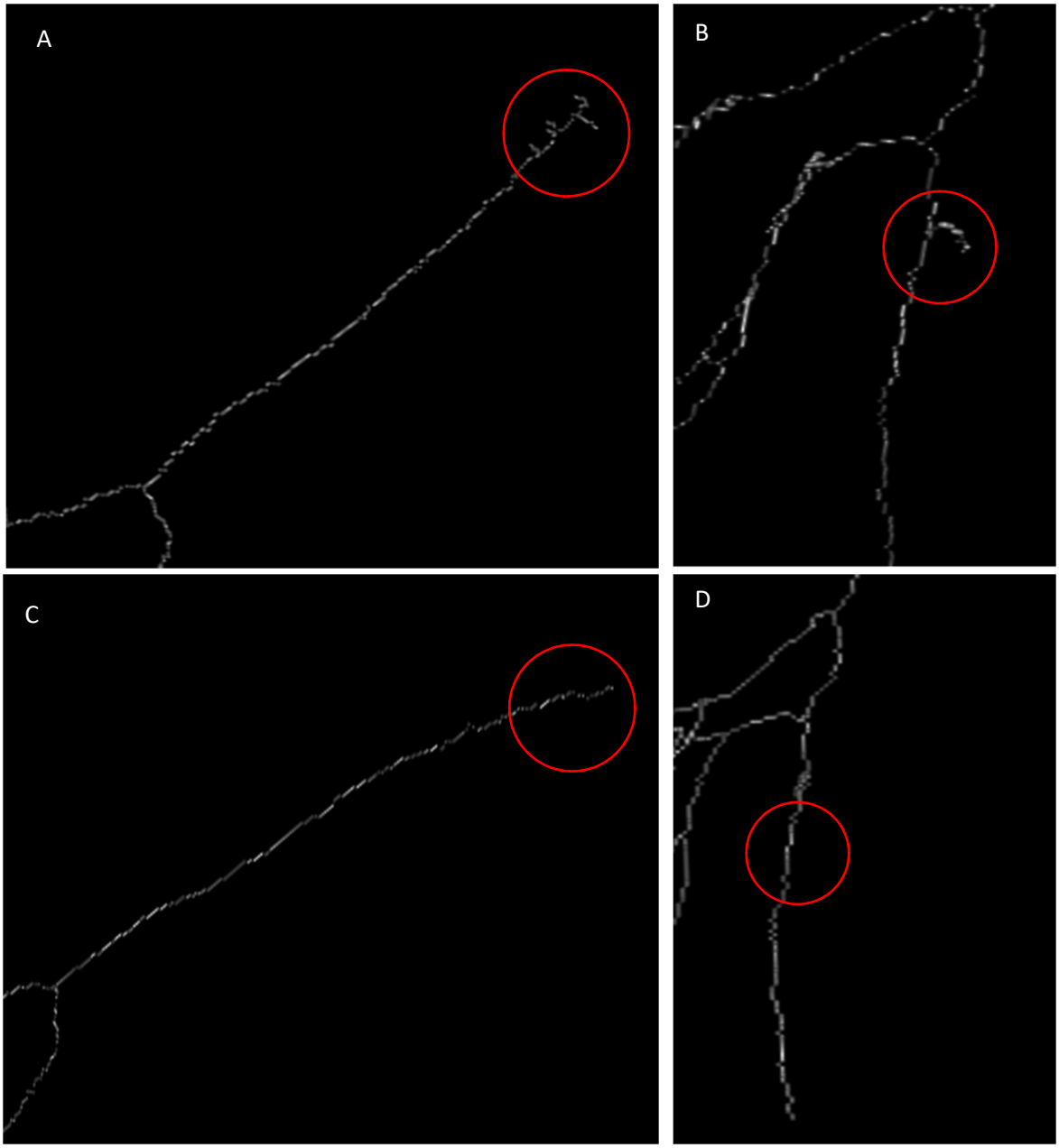


Figure 2.6 Examples of spurs at the level of the trachea (A) and at the level of a segmental bronchus (B), which can be resolved using the Opening filter (C), (D)

### 2.1.3. Morphometry Analysis

This step concerns the extraction and measurement of morphological parameters of airways. The procedure followed to accomplish this step comprises:

1. Creation of a Tree data structure starting from the centreline.
2. Labelling.
3. Identification of specific points in each centreline segments where make the measurements.
4. For each point considered and one point per time, resample the 3D image to an oblique section centred in that specific point and orthogonal to the centreline segment considered.
5. Calculate the relevant morphological parameters working on the 2D resample image, considering one point per time.

#### 2.1.3.1. Creation Of The Tree Data Structure

Before proceeding on take the measurements is necessary to create a suitable data structure. The data structure is used to store and organize data in such way to be easily accessed, updated and processed[r].

As already seen, the tracheo-bronchial tree can be intended as a tree having the trachea as root which branches in several ramifications, the airways.

So, the Tree data structure is the most suitable one to organize data. A Tree is a non-linear data structure defined as a collection of objects known as nodes that are linked together in a hierarchical configuration.

Every tree has one root node, which is the topmost node and the one without any parent. A node containing any sub-nodes is said to be the parent of that sub-nodes.

The descendant of any node is the child node and nodes having the same parents are named siblings. The node of the tree without any child node is called a leaf node and it is the bottom-most node of the tree.

So in the tree data structure there will be a node for each airway segment identified in the centreline and the relevant information regarding each segment will be saved in the corresponding node[s] , an example is reported in Fig. 2.7.

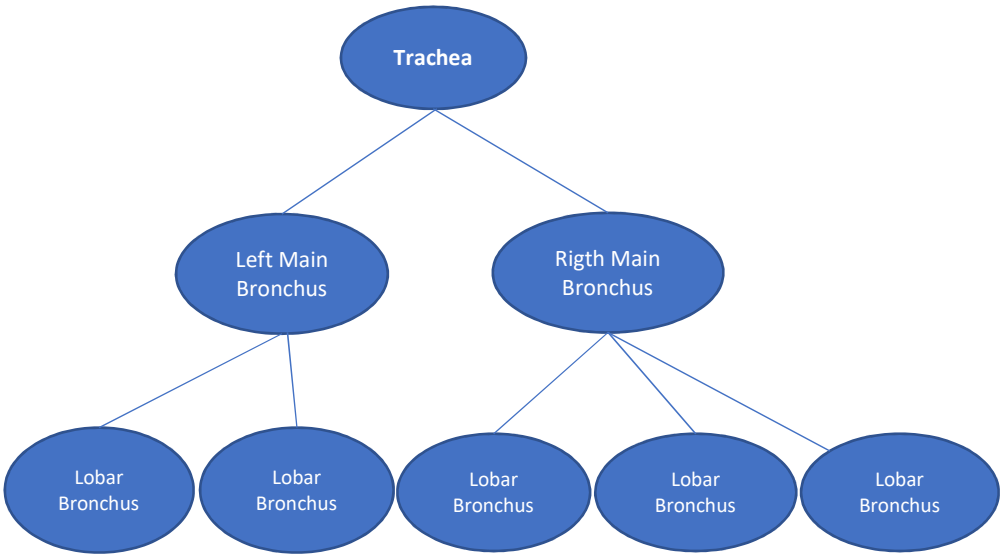


Figure 2.7 Example of the created tree data structure illustrated up to the second generation of bronchus.

The first necessary step for the creation of the tree data structure is the identification of the branch-points (or bifurcation points), which has been accomplished by Python library Skan, designed to analyse skeleton's images[45].

Each airway segment, called also branch, belonging to the centreline has two branch-points which correspond to the two points at the extremity (Fig. 2.8). The branch-point is defined as end-point if in that point the skeleton ends; it is a junction if in that point three or more skeleton branches meet (or evenly if in that point a branch split into two or more branches)[t].

Using the functions implemented in this library it was possible to retrieve a Data Frame with one row per branch and one column for each relevant information about the branch, which are:

- The branch type, which is coded by number: 0 if both its branch-points are endpoint and so the branch is an isolated branch type; 1 if one branch point is a junction and the other one is an end-point; 2 if both the branch-points are junctions.
- The coordinates of its two branch-points, in natural space.
- The unique IDs of the branch-points.
- The branch distance as sum of the distances along path nodes between two nodes in natural scale.
- The Euclidean distance between the branch-points.
- The coordinates in image space (pixels).
- The unique ID of the skeleton that the branch belongs to.

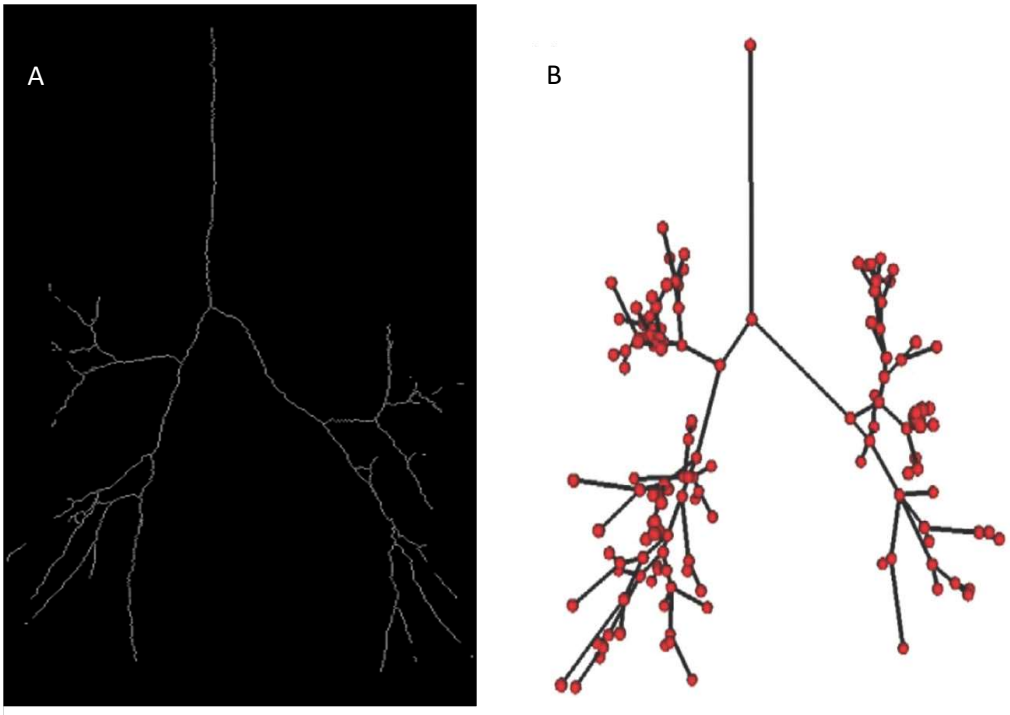


Figure 2.8 A) result of the skeletonization procedure; B) example of branch-points identification (in red) using Skan library [47]

The branches having a branch type coded as 0 are discarded as not useful for the creation of the tree data structure as they may be the consequence of the application the opening operation, which disconnects small branches segment from the principal airway tree structure.

The tree data structure has been implemented using the Python library called Treelib[u] which guarantee:

- efficient operation of node searching;
- common tree operations like traversing, insertion, deletion of nodes;
- the storing of all the wanted data in each node.

In order to create the tree hierarchical structure, a recursive function have been implemented, which exploit the data frame containing the relevant information of each branch. Two branches in a relationship parent-child have a branch-point in common, which is recognizable by its unique ID in the data frame.

One of the major advantages of building this tree data structure is to create an airways tree model in which store information about individual airway branches easily [57].

At this point the available information stored in each node are:

- the coordinates of its branching points;
- the coordinates of each point constituting the branch that the node represents;
- the length of the segment branch.

#### 2.1.3.2. Labelling

In this work the airways up to the third generation have been labelled taking into consideration the geometry characteristics and the hierarchical organization of the trachea-bronchial tree. Indeed for the first three generations, the airway branching pattern is standard [46] .

The trachea splits in the left and right main bronchi (LMB and RMB) leading to the left and right lungs. Beneath the LMB and RMB, bronchi lead to the left and right upper lobes, right middle lobe, and the left and right lower lobes. In the right lung, the right upper lobe (RUL) branch leads to the upper lobe and the Bronchus Intermedius (BronchInt) leads to the middle lobes and lower lobes, in which the lung is fed by the right middle lobe (RML) branch and by the right lower lobe (RLL) branch respectively. In the left lung, the left upper lobe (LUL) branch and the left lower lobe (LLL) feed the upper lobe and the lower lobe respectively.

Taking into consideration this hierarchical organization and these geometrical features the labelling has been performed. So the trachea is easily recognizable as root of the tree. The LMB and RMB are the first generation of airways and stay on the left and on the right part of the image respectively. The RUL is identified by checking among the second generation of airway branches belonging to the right lung the one having the middle point with the highest z coordinate. Similarly, for the BronchInt, checking for the one with the lowest z coordinate. Considering again the airways position inside the lung, the differentiation between the RML and RLL branch was possible. The same process is repeated for the left lung.

Beyond this depth, the branching variabilities are more consistent. So, the labelling has been performed considering just the hierarchy and the lobe fed by the airways, without differentiating among airways belonging to the same generation. An example of the result obtain for one image series is illustrated in Fig. 2.9.

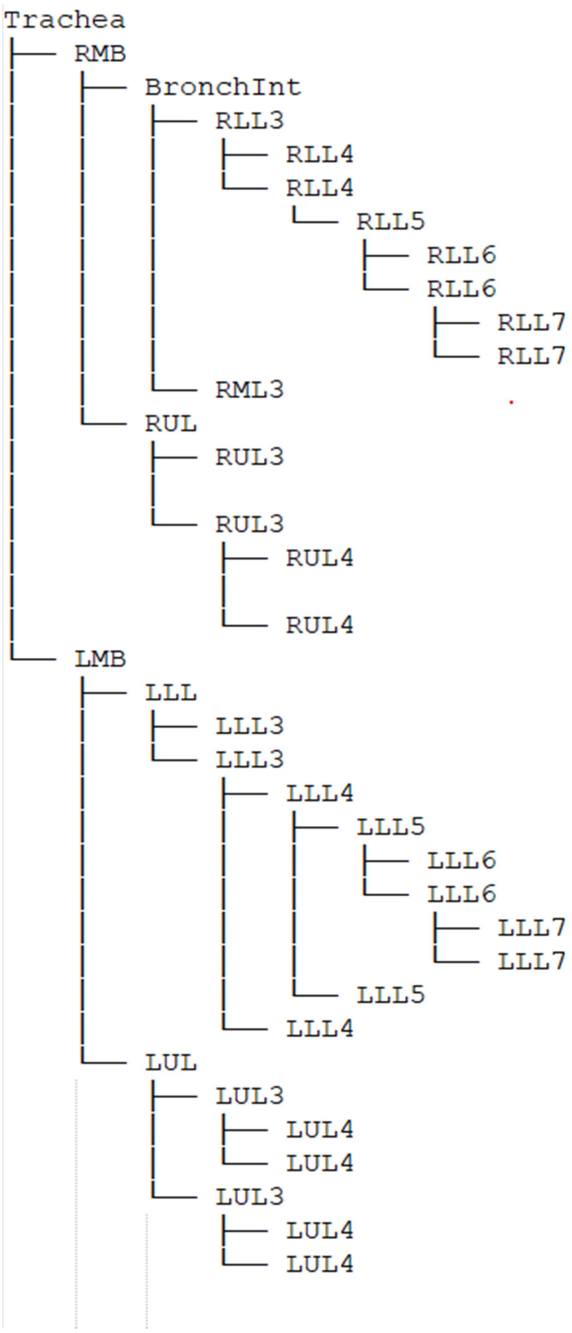


Figure 2.9 illustration of the hierarchical structure obtained. The name assigned to each airway represents the lobe reached by that airway, the number represents the airway generation.

#### 2.1.3.3. Points Selection For Measurements

The measurements have been initially performed on three points on each segment: the middle point; two segments equally distant from the middle point, but not too much close to the bifurcation point.

Points coincident or close to the bifurcations generated error during the resampling process to extract the oblique slice, as it was inevitable to consider also adjacent the segment.

For comparing the healthy and the asthmatic groups, just the middle point measurements have been used, as considered to be the most reliable.

#### 2.1.3.4. Extraction Of The Orthogonal 2D Section From The 3D Image

Before proceeding with the measurements of the relevant morphological parameters in correspondence of the selected point, a 2D section of the airway on a plane perpendicular to the centreline and centered in the specific point needs to be extracted.

The extraction of this 2D image is necessary to avoid error due to the oblique orientation of the airways with respect to the axial plane of the slice. Indeed, the angle of orientation at which an airway is imaged, relative to the scan plane, can affect the measurements. Any deviation from the orthogonal direction with respect to the axial plane leads to an overestimation of airway wall thickness and underestimation of airway lumen[47] . This effect occurs in all the airways and it is more pronounced in those imaged parallel to the scanner, as visible in Fig. 2.10.

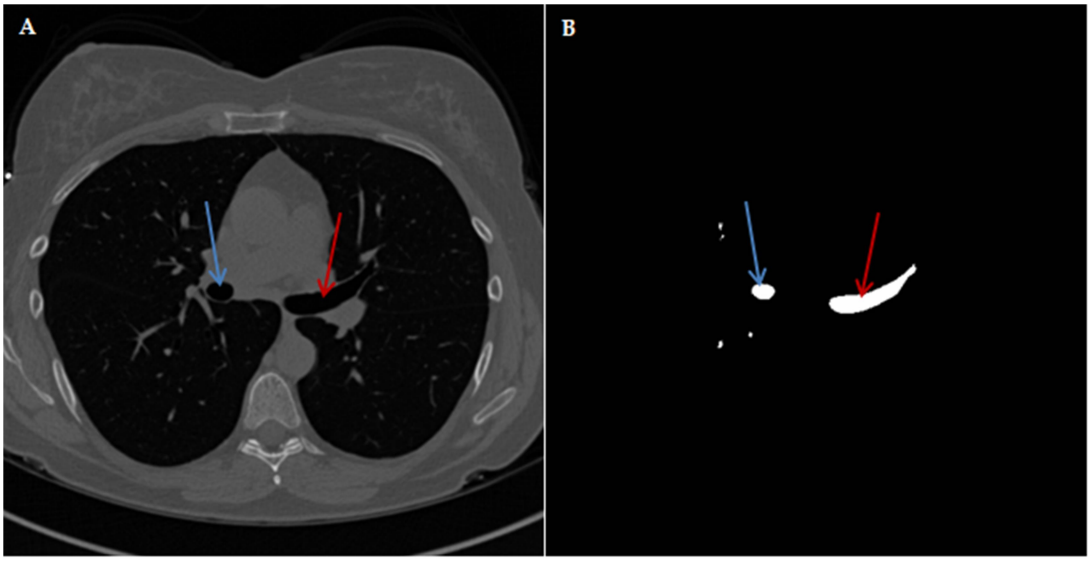


Figure 2.10 Example of airways that run apparently perpendicular to the axial plane (blue arrow) and example of airway imaged almost parallel on the axial plane (red arrow) and in this case a section of the airway orthogonal to the centreline on both the (A) original and (B) segmented image is essential to retrieve morphological parameters.

In order to limit these effects caused by an oblique orientation of the airways, many studies have only measured airways that lie orthogonally to the scanner plane, excluding in this way the majority of airways.

A superior approach, that is also adopted in this work, requires to resample the data to ''re-orient'' the slice to be perpendicular to the centreline of the airway.

The function implemented to obtain an oblique 2D section is taken from the paper of Mueller et al. [48], which describes the ITK implementation of a transform initializer to produce a rigid 3-D transform able to center a given point on an arbitrary plane, which is perpendicular to the centreline in this application. The resultant transform is used to obtain a single 2-D slice from the 3-D image.

The procedure carried out in this paper uses the Resample Image Filter to resample the input 3D image and produce a one slice 2-D image by linear interpolation. Through this filter a suitable 3D transform is applied to the input image. This transform is initialized by specifying the centred plane, which is retrieved by providing the center point and the direction as inputs. The center point, which

corresponds to the centreline point where getting the measurements, represents the center of the transform and it is used to calculate the translator operator needed to translate the center point to the center of the final image. The direction is calculated as the difference between the coordinates of the center point and another point belonging to centreline which lies three position ahead the center point.

Finally, the Extract Filter is used to extract the final 2D image, which depicts, in its center, the orthogonal section of the selected airways.

This procedure is performed one point per time and it is applied both on the 3D original image in grayscale and on the 3D binary image depicting the result of the segmentation. An example of the result obtain is illustrated in Fig.2.11.

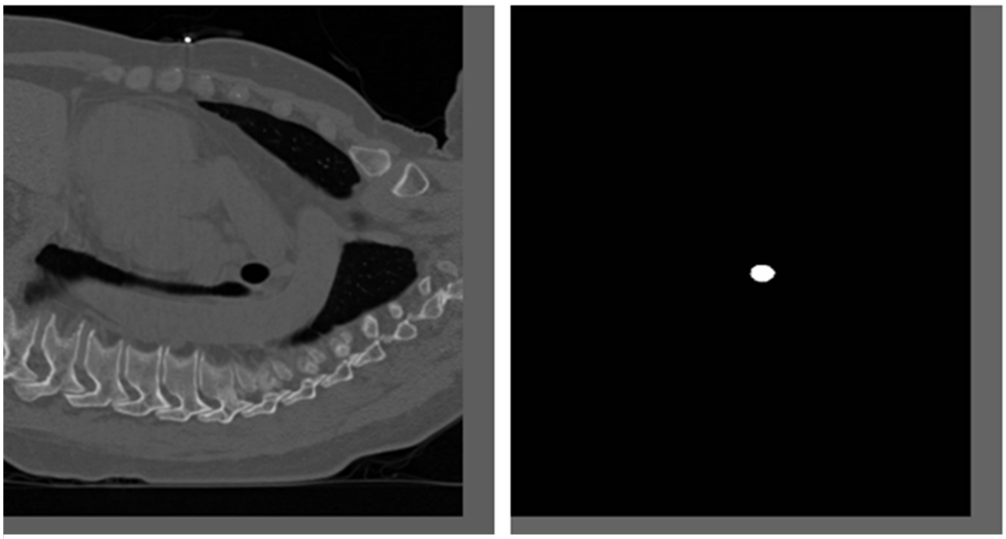

Figure 2.11 example of final 2D images obtained after the resample followed by the extraction procedure applied on the 3D original image and on the 3D segmented image.

A segmentation process is also applied on the 2D image thus obtained from the 3D binary image to identify just the airway depicted in the center of the image, which is the one of interest, and discard other airways potentially depicted in other parts of the image because taken into consideration during the resampling.

Once the orthogonal section of the airway is retrieved for one point it is possible to proceed with the measurements.

### 2.1.3.5. Measurements Of Morphological Parameters

On the resampled 2D images, the relevant airway structures are segmented.

The parameters retrieved by the algorithm are (Fig. 2.12):

- Lumen area;
- Total area;
- Bronchial wall area;
- Wall percentage area;
- Major and Minor inner diameter;
- Major and Minor outer diameter;
- Wall thickness.

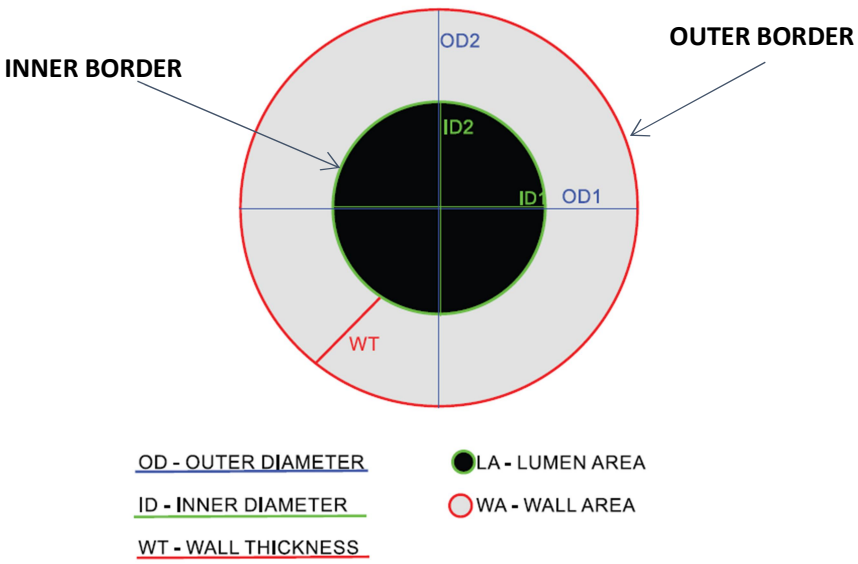


Figure 2.12 recall of the relevant morphological parameters [24]

**LUMEN AREA:**

The lumen area is retrieved by applying the resampling procedure to the 3D binary image related to the segmentation of the lumen area. A binary 2D image is obtained depicting on its center the lumen area which is calculated and expressed in mm^2.

**TOTAL AREA:**

The problem of airway area segmentation is related to the correct identification of the airway wall borders.

In literature, many techniques can be found about borders identification and most of them are based on either edge detection algorithms or FWHM principle. In this work, an attempt was made to apply these techniques but without obtaining a satisfactory results, as they failed in identifying the outer border, especially in those situations in which the airways were, even only partially, surrounded by soft tissues. An example of this situation is reported in Fig 2.13 .

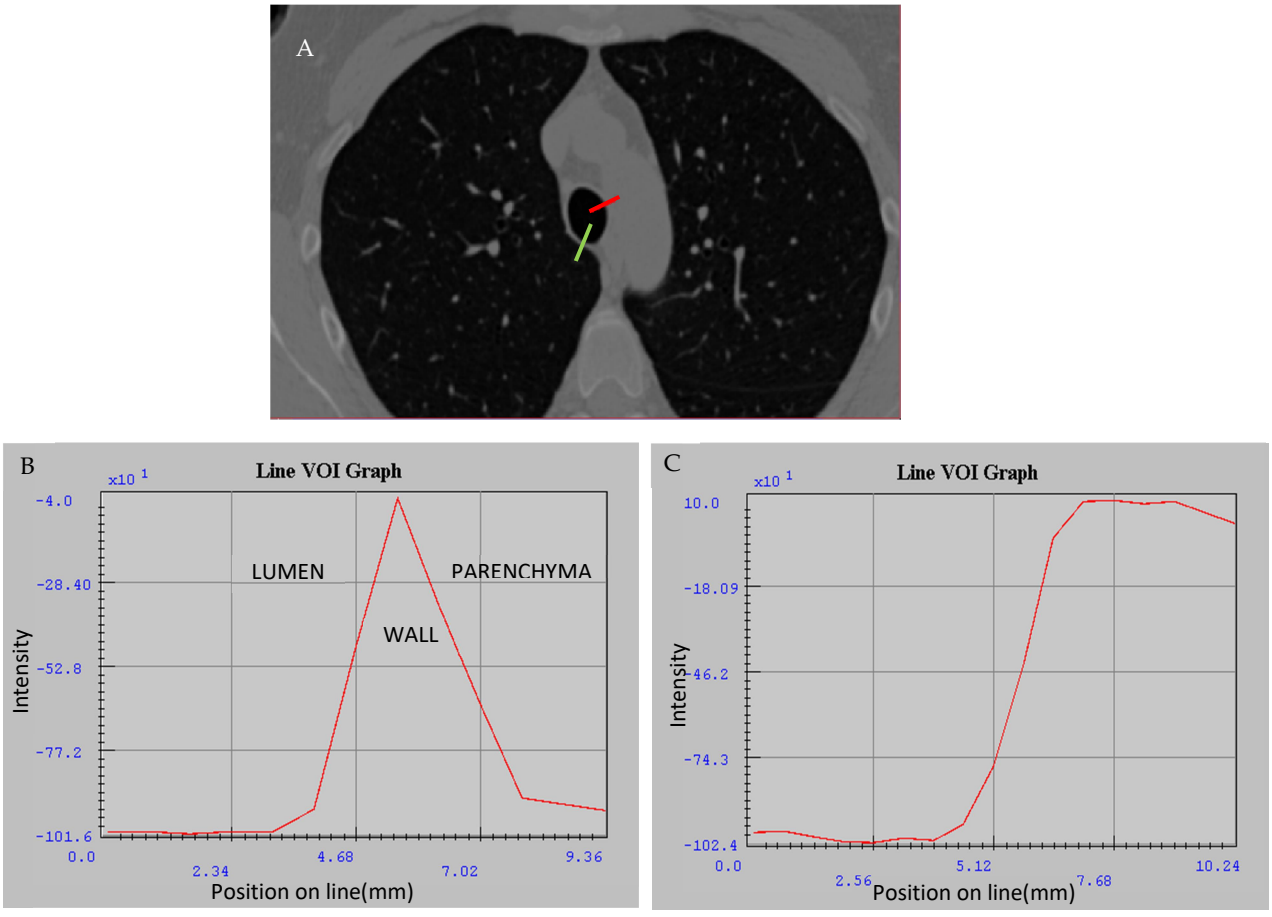


Figure 2.13 Example of airway partially surrounded by soft tissue (A). Two intensity profiles are reported, related to green segment (B) and red segment (C). It is evident how in B it is possible to identify the inner and outer border according to a change in pixels intensity; instead in C just the internal border can be identified, concerning the outer border, no evident change is noticeable.

In this work, we implemented an iterative Dilation operation process.

The dilation is iteratively applied to the segmented airway lumen obtained in the previous step by using a round kernel. At each iteration a new dilatation is performed and the mean intensity value of the corresponding pixels in the original image is calculated. The iterative process is stopped when the mean value decreases by 20% with respect to the previous iteration and the previous iteration is maintained valid for the calculation of the total area. An example of this iterative process is illustrated in Fig. 2.14.

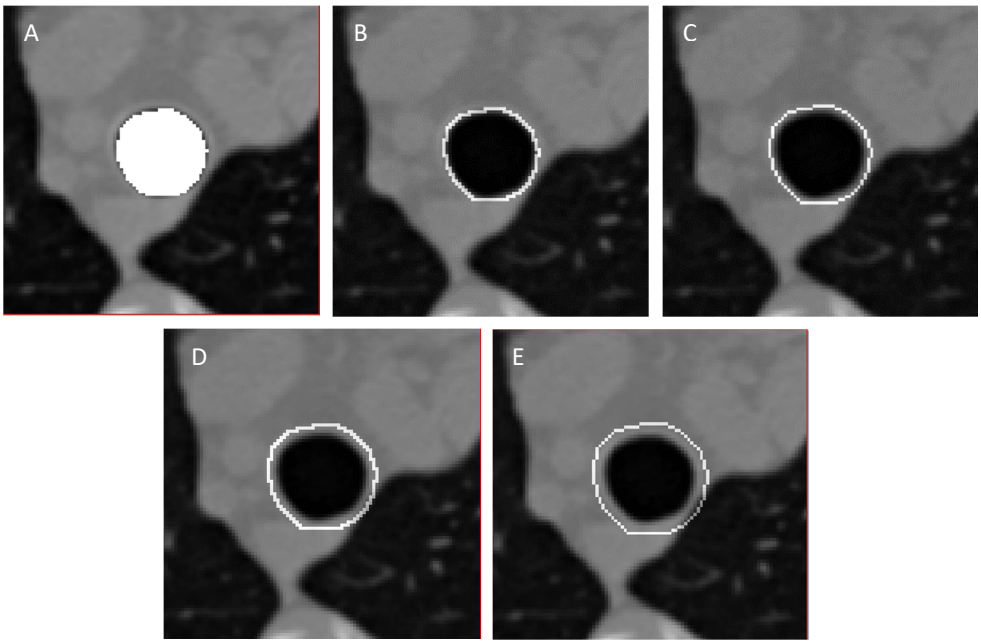


Figure 2.14 example of the iterative process of dilatation: A) the starting point is the airway lumen already segmented; B) annulus obtained by the difference between the dilated lumen area and the previous one, and in correspondence of the white pixels in the gray-scale image the mean intensity value is calculated; C),D) the iterative process continues, until the parenchyma is reached (E).

The hypothesis is the following: in correspondence of the bronchial wall the mean intensity value is comparable to that of the soft tissue (about 50HU), whereas, out of the bronchial wall, the mean intensity value suddenly decreases as the lung parenchyma is included (about -800HU). So, a mean intensity drop by 20%, means

that the outer wall border has been crossed and that the parenchyma starts to be comprised in the dilatation.

A maximum number of iterations is anyway set to deal with situations where the airway is completely surrounded by soft tissue and so the outer border is not recognizable at all.

This situation is depicted in the Fig. 2.15, showing that no evident change in pixel intensity value is present.

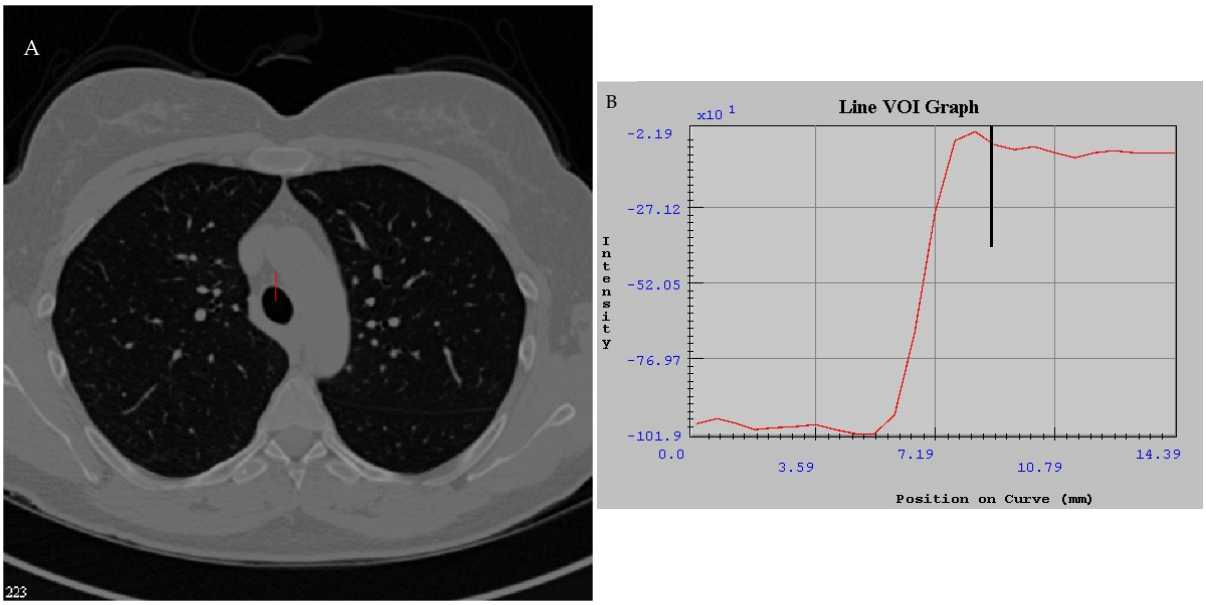


Figure 2.15 A) example of an airway completely surrounded by soft tissue in which a decrease of the 20% may not be detected. B) In correspondence of the fastest decrease in the mean intensity value (black line) there is the outer border.

In this work the number of maximum iterations is arbitrary set to five.

Moreover, if the maximum number of iterations is reached, another strategy has been designed for the outer border identification. During the iterative process, each mean intensity value corresponding to each new dilatation is memorized in a list. The difference between a mean intensity value and its adjacent value in the previous position in the list is calculated for each member of the list, thus obtaining five values of differences. The minimum value among these differences is searched and the corresponding iteration is selected as the one in which there is the fastest decrease in

the mean intensity value, and is selected as the most suitable for the outer border identification.

Once the outer border has been segmented, the total area is calculated and expressed in mm^2.

**BRONCHIAL WALL AREA and WALL PERCENTAGE AREA:**

The bronchial wall area is finally calculated as the difference between the total area and the lumen area. The binary image representing the segmentation of the bronchial wall is also retrieved (Fig. 2.16 ) and used in the following step. The wall percentage area (WA%) is calculated as: (EdgeArea/TotalArea) * 100.

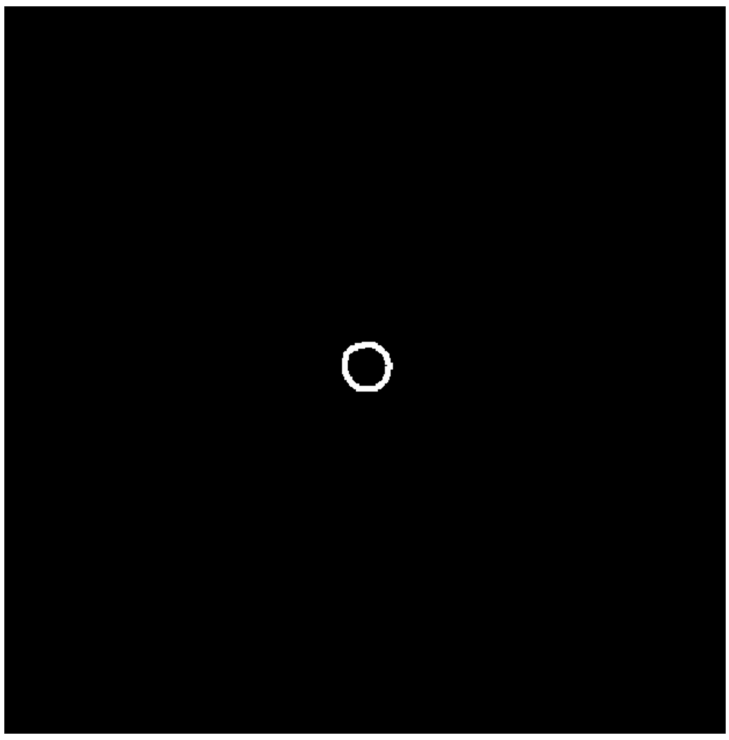

Figure 2.16 example of a bronchial wall segmentation

**WALL THICKNESS**

The wall thickness is calculated taking into consideration the binary image depicting the bronchial-wall area, retrieved as output from the previous step. The

measurement is performed by tracing ray segment starting from the center of the image, as illustrated in Fig. 2.17. When the segment crosses the internal and the outer white borders, the x and y coordinates of each crossing points, p1 and p2 respectively, are retrieved. The differences between the coordinates of the two points are calculated and multiplied by the image spacing. Finally, the wall thickness is retrieved by calculating the square root of the sum of the differences, according to the Pitagora theorem.

A total of 36 ray segments have been traced, one every 10 degree and for each segment a value of wall thickness is calculated. Then these 36 values are averaged to obtain a mean value of wall thickness in millimeters related to the considered airway.

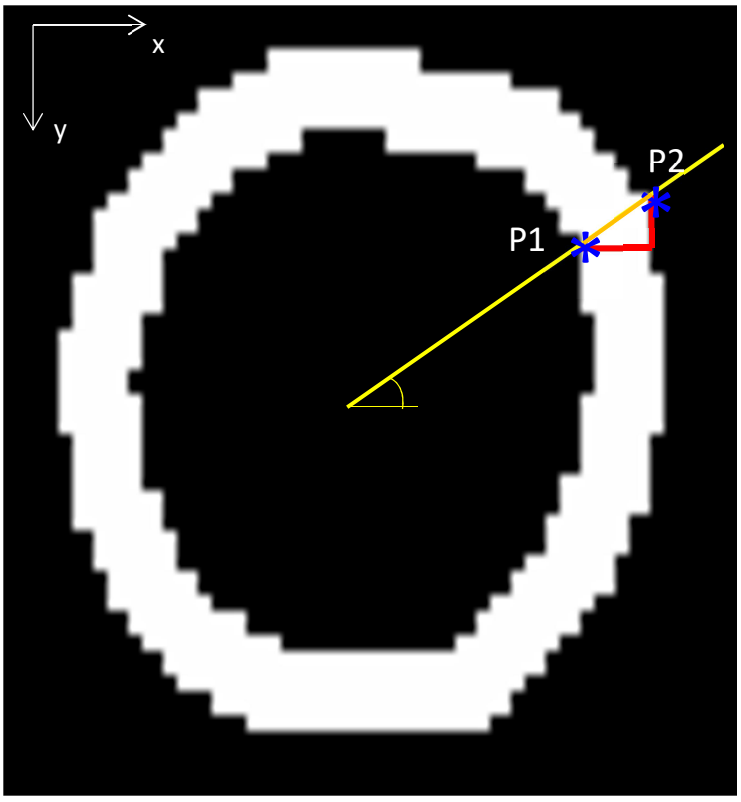


Figure 2.17 illustration of the procedure: the figure represents the zoomed image of the bronchial-wall area; a ray (yellow) with a certain inclination angle, starts from the center of the image, which correspond to the center of the airway, crosses the bronchial wall in two point, P1 and P2 (blue star); the differences between the x coordinates and y coordinates (red segments) of the two points are calculated and then used to retrieve the wall thickness through the Pitagora theorem

**MAJOR AND MINOR INNER AND OUTER DIAMETER:**

These parameters can be easily retrieved once segmented the internal lumen area and the total area by using the designed function already present in the 'scikit-image' [44] library of Python. 'Scikit-image' is a collection of algorithms for image processing containing a module called 'measure' useful to measure properties of objects present in binary images as the major and minor diameter of image regions having an elliptic shape. In particular, the parameters used for the further analysis are the mean inner diameter and the mean outer diameter, calculated as the mean between the major and minor diameter. Another parameter considered is the ratio between the wall thickness (WT) and the mean outer diameter (OD).

## 2.2. Validation Procedure

The developed algorithm has been validated by comparing the measurements retrieved using the algorithm and the same measurements obtained manually.

Ten points for each healthy patient are randomly selected. In those points the measurements of total area and lumen area are retrieved both automatically, using the algorithm just implemented, and by manual segmentation using the software MIPAV[v].

Using MIPAV it is possible to open the original DICOM file image in grayscale, select the point previously randomly identified using a point VOI, apply the same transformation retrieved during the resample process, and manual segment the total area and lumen area of the airway section displayed. This procedure is illustrated in Figure 2.18.

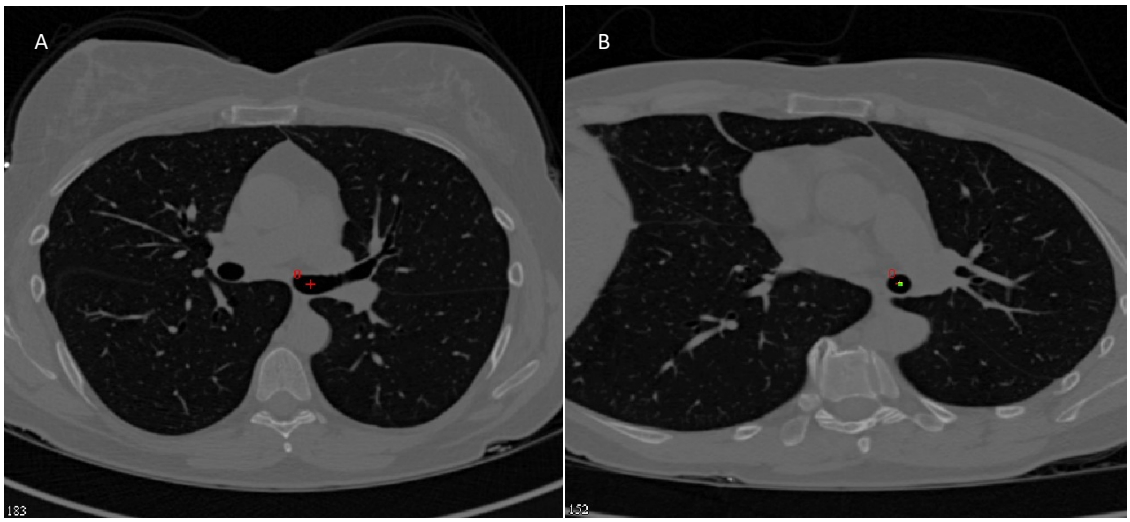


Figure 2.18 A) Original grayscale image open with MIPAV where a point VOI is drawn in correspondence of a specific point; B) on the original image the roto-translational transform specific for the selected point is applied and in correspondence of the point VOI now we visualise the orthogonal section of the airway.

Once obtain the airway section is possible to proceed with the manual segmentation using suitable MIPAV tools. The lumen area is detected by drawing a levelset VOI positioning the mouse cursor inside the airway lumen. The total area is detected by drawing a polyline VOI in correspondence of the outer border. The identification of these area is depicted in Fig. 2.19.

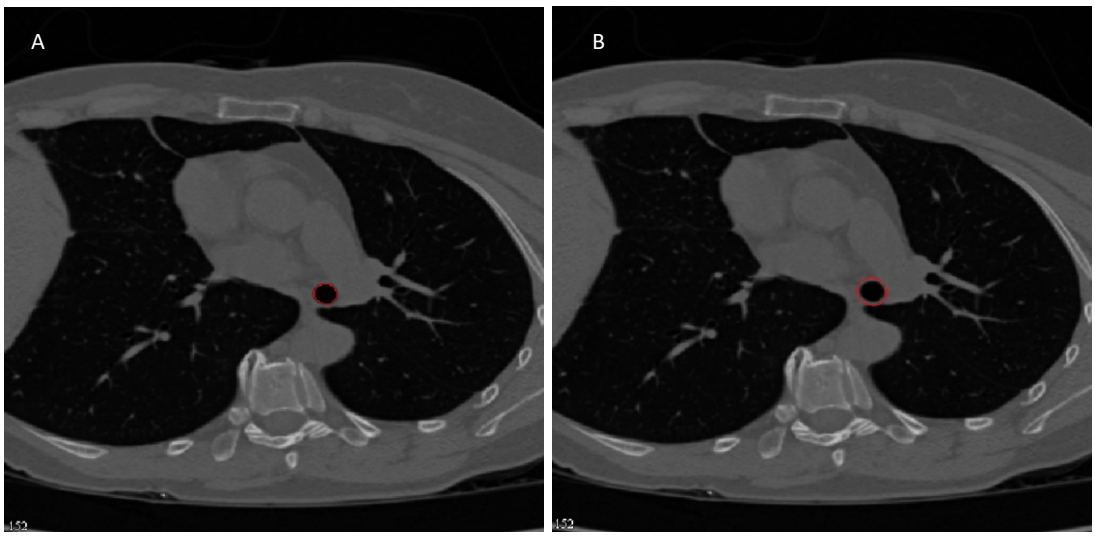


Figure 2.19 A) identification of airway lumen area and B) identification of the total area by drawing the suitable VOIs.

The area contained in the depicted VOIs is calculated using the appropriate function in MIPAV. This procedure is repeated for all the 50 points randomly selected.

So we obtain 50 measurements of areas automatically retrieved using the design algorithm and 50 measurements obtain by manual segmentation for both the lumen area and the total area. The comparison between the 50 automatically computed measurements and the 50 manually traced measurements is performed by calculating the Linear Regression and the R-square and by retrieving the Bland Altman Plot.

## 2.3. Comparison between Healthy And Asthmatic Subjects

The validated algorithm is applied in asthma patients and the relevant morphological parameters have been calculated for comparison to the healthy subjects.

In this work all the airways retrieved, of both the right and the left lung, for each healthy and asthmatic subjects are considered for the measurements. The points where the measurements have been calculated for the comparison, are the middle points of each airway. It was decided to not consider the other two points equally distant from the middle point, as in some segments with a shorter length the measurements retrieved in those points resulted to be erroneous as too close to the bifurcation points.

Before proceeding with the analysis, the data have been re-organized:

- The five different morphological parameters are considered separately.

- The measurements of right and left lungs are at first considered separated and then mixed together.
- The data are organized in column, each column containing the data related to the same generation of airway of all the subjects, maintaining the healthy and asthmatic groups separated.

The comparison between the same generations in healthy and asthmatic subjects is performed using a t-test, if the data are normally distributed, or a Mann-Whitney test otherwise. The normality test (Shapiro-Wilk) is initially performed for each generation. P-values below 0,05 were considered statistically significant.

This analysis is performed for all the morphological parameters measured: lumen area, total area, bronchial-wall area, wall area percentage, inner and outer diameter and wall thickness.

# 3 Results and Discussion

## 3.1. Qualitative Evaluation Of The Algorithm

The segmentation results are visually evaluated in order to check possibly leakages of the airways on the lung parenchyma (Fig. 3.1).

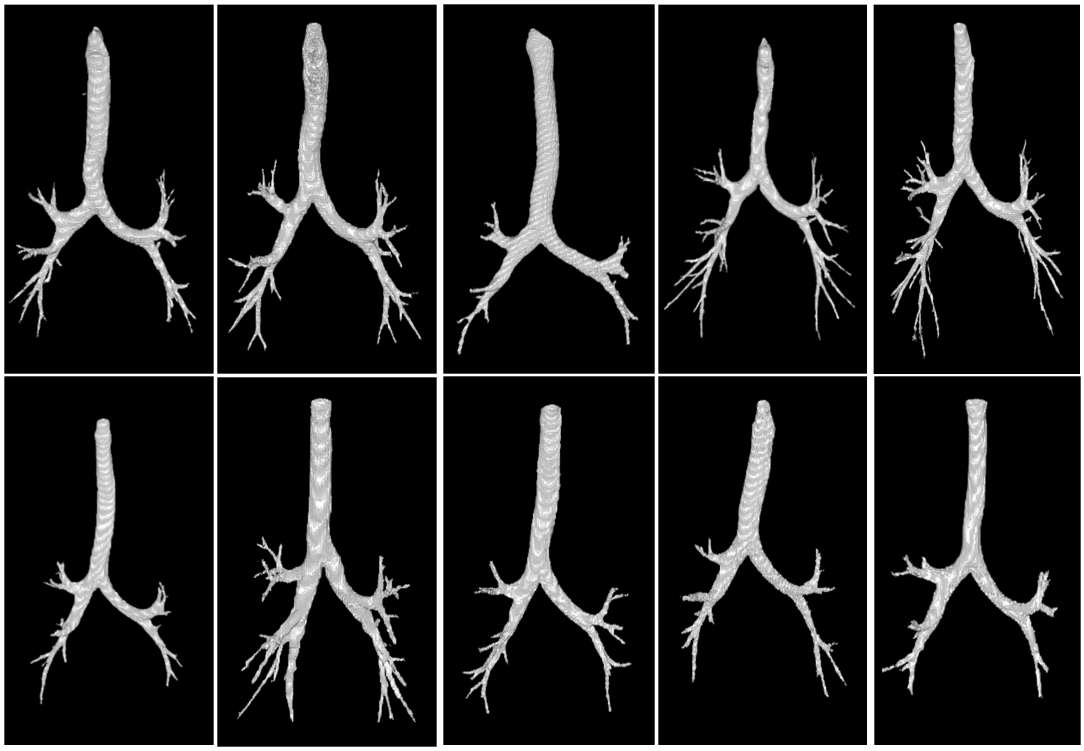

Figure 3.1 result of segmentation process for the healthy subjects (first row) and asthmatic subjects (second row)

The number of airways generation reached during the segmentation varies among subjects, and between the right and left lung of the same subject. All the generations up to the 4$^{th}$ were reached for all the subjects, the 5$^{th}$ generation was reached in 9 of 10 subjects, the 6$^{th}$ generation was reached in 7 of 10 subjects and the 7$^{th}$ was reached

in 3 of 10 subjects. Moreover, on average the proposed algorithm identified 28 ± 6.5 anatomically segments per tree (mean ± standard deviation).

The generation depth reached by the segmentation algorithm implemented in this thesis work is actually lower if compared to other studies, that can identify up to the ninth [24] or tenth [10][3] generation.

An explanation for this lack in identifying deeper generations can be found considering the method applied in the present work for the accurate identification of the centreline from the airways lumen segmentation.

Indeed, in order to obtain a clean centreline without spurs or defects, a closing filter followed by an opening filter is applied to the 3D binary image depicting the airway lumen. In particular, the opening operation is shown to be effective for noise removal, but leads also to the disconnection of small branch segments from the principal airway tree structure and this may be the cause of a lower depth of generations achieved by the segmentation algorithm compared to other studies.

## 3.2. Validation Of The Algorithm

The validation procedure is performed to evaluate the accuracy of the implemented algorithm.

The measurements automatically retrieved by the algorithm are compared to the measurements obtained by the manual segmentation performed using MIPAV. For this procedure just the healthy subjects are taken into account.

We performed a linear regression analysis, in which the manual measurement is the independent variable, and the algorithm measurement is the dependent one.

The Bland-Altman plot is also represented, to evaluate the agreement between the two quantitative measurements. The y-axis shows the differences between the two groups of measurements and so represents the measurement error, the x-axis shows

the arithmetic means of the two groups of measurements. The upper and lower limits are shown and represent the confidence interval of the mean of the differences, the values out of this range are outliers. The mean of the differences is also calculated to verify the presence of possibly systematic errors.

This validation analysis is applied to the lumen area and total area measurements, as all the other parameters are computed starting from these two measurements.

The results thus obtained concerning the Lumen area and Total area are reported in Fig. 3.2.

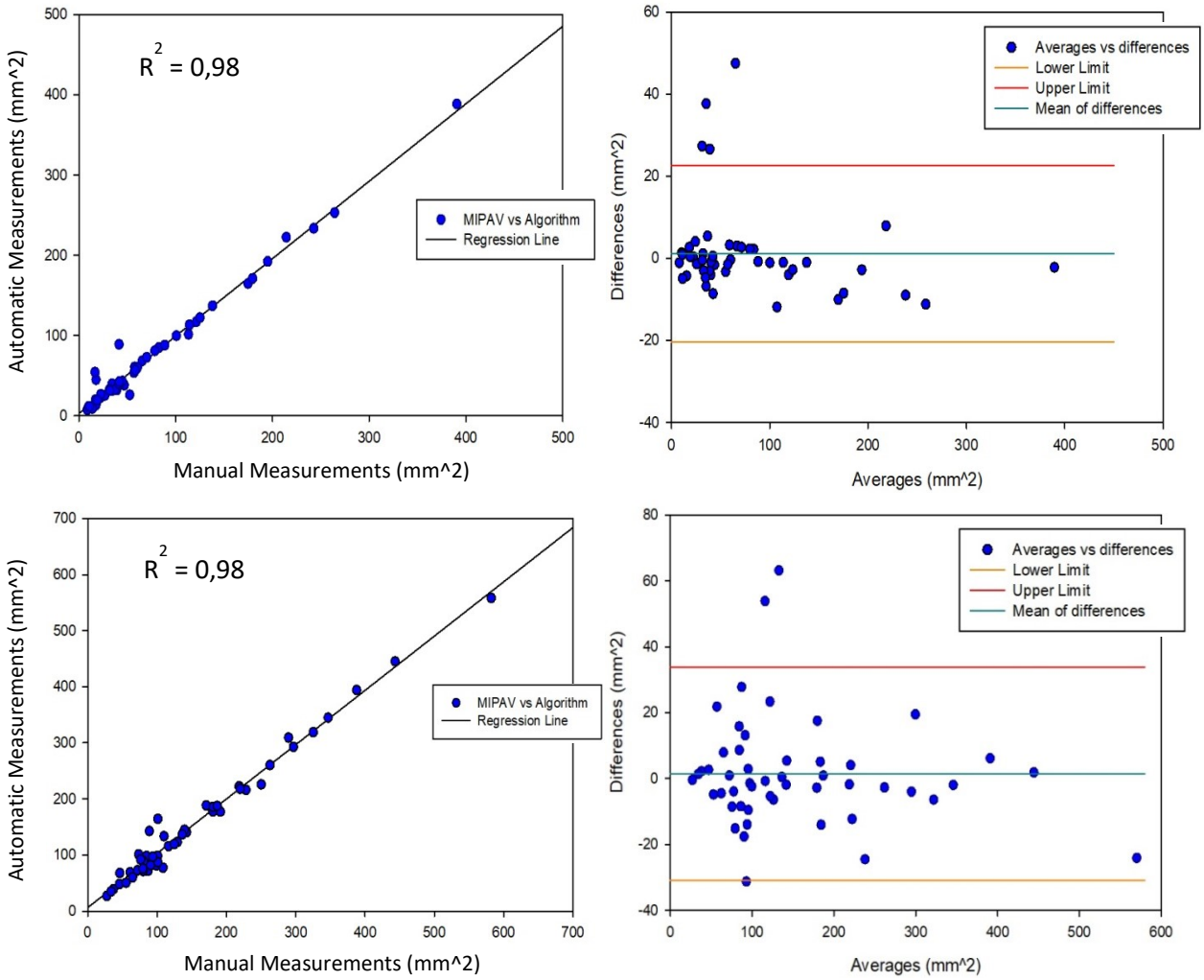


Figure 3.2 Regression analysis and Bland-Altman plots of Lumen Area (first row) and Total Area (second row)

The results show that for both the total and lumen area the data are not dispersed around the line of regression, except for few points in correspondence of the lower values. The determination coefficient is very close to 1 demonstrating that the analysed quantities just slightly deviate on average from regression line. These results demonstrate a strong linear relationship between the measurements manually retrieved by MIPAV and the ones automatically retrieved by the algorithm.

The Bland-Altman plot shows that the data are dispersed around the zero, the majority of them lie within the range defined by the upper and lower limits demonstrating a strong agreement between the two methods of measurements. There are four and three measurements concerning the lumen area and total area respectively which are out of the range. In those points the presence of two airways very close to each other was observed. In this case the algorithm failed in identifying the border of separation and so in distinguishing the two different airways. An example of this error is reported in Fig. 3.3. The measurement calculated by the algorithm due to this error is about the double of what it should be, that is because the two close airways are considered as one.

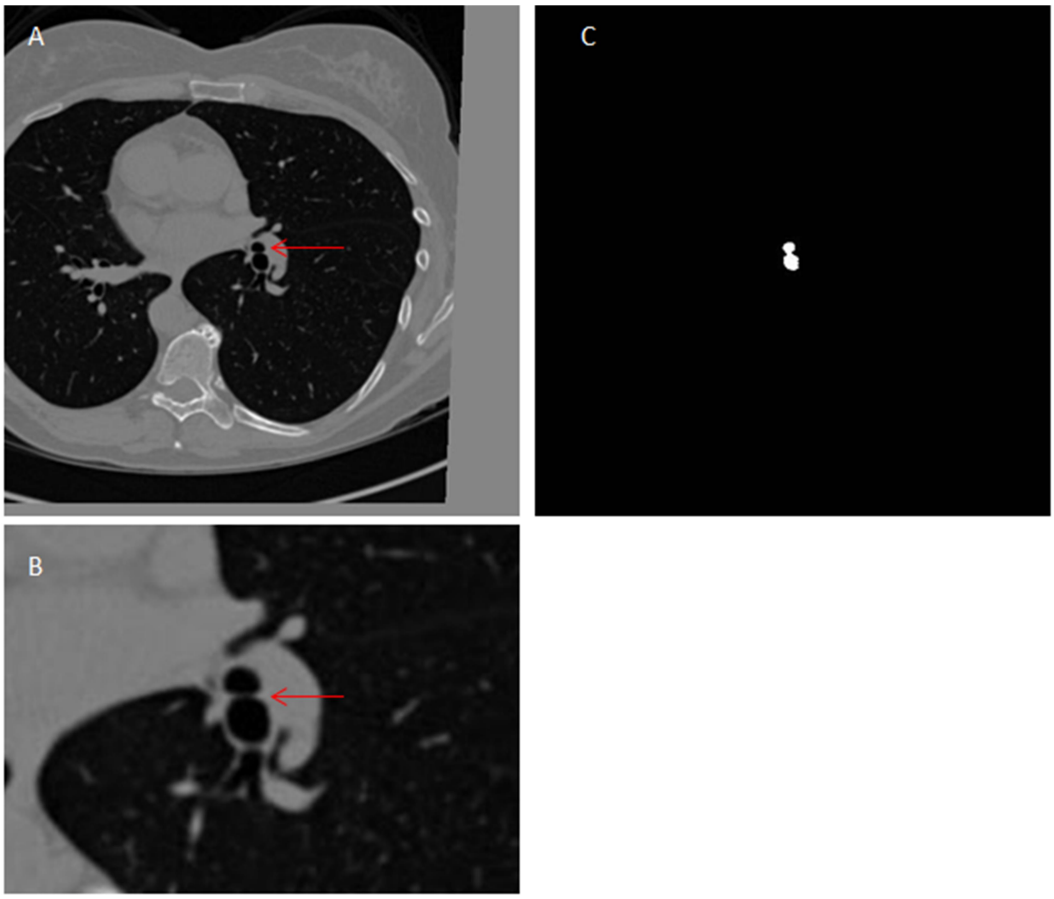


Figure 3.3 example of two airways very close to each other in the A) resampled original image; B) the border of separation is not very visible and so the algorithm in this case fails to correctly segment two different airways (C) and so to retrieve the correct measurements.

Some additional effort that could be done to solve the problem depicted in Fig.3.3 is to apply some filter for the edge enhancement on the original 3D image to make the border of separation between two close airways more detectable by the algorithm or apply some additional segmentation algorithm, like the watershed that allows to separate different objects which overlapped, on the 2D resampled binary image.

We also evaluated the upper and the lower limits of the Bland Altman plots by discarding the outliers (Figure 3.4).

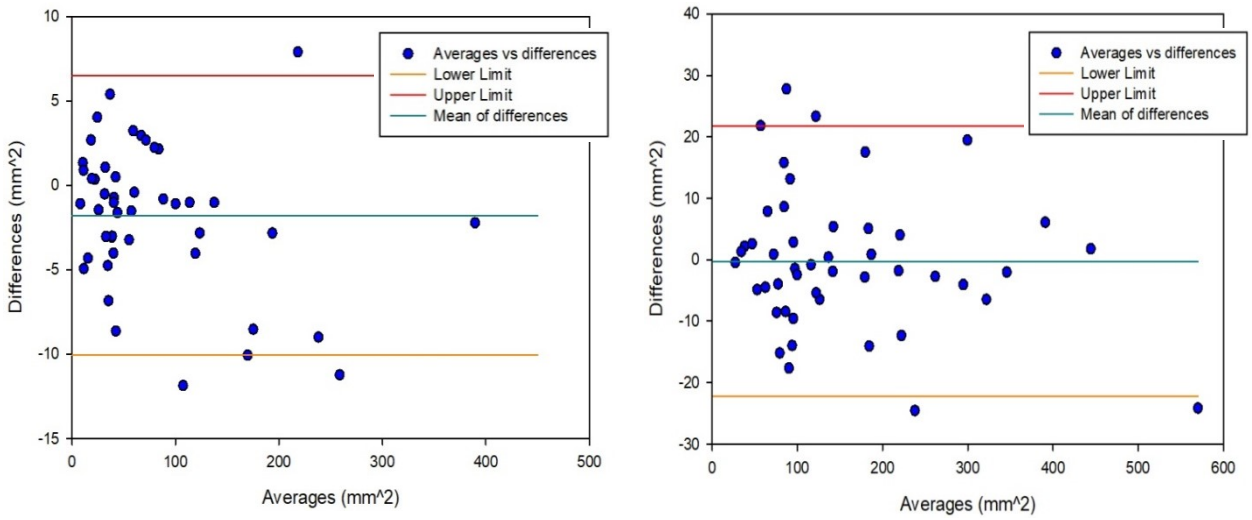


Figure 3.4 Bland-Altman plots without the outliers for the Lumen area (left) and the Total area (right)

In particular, considering the lumen area, the new range is between -10.07mm$^2$ and 6.48mm$^2$, while the previous one is between -20.40mm$^2$ and 22.66mm$^2$. Considering the total area, the new range is between -22.21mm$^2$ and 21.72mm$^2$, while the previous one is between -30.91mm$^2$ and 33.89mm$^2$. The mean difference of the measured total area is equal to -0.24mm$^2$. Instead, the mean difference of the measured lumen area is equal to -1.8mm$^2$. So, there is a systematic error related to the algorithm, that slightly underestimates the value of lumen area.

The results of the validation procedure, considering both the regression analysis and the Bland-Altman plot demonstrate that the algorithm implemented in this work can be used to correctly predict the relevant parameters concerning the morphology of the airways. Some additional efforts are required to avoid the erroneous measurements in those situations depicted in Fig.3.3, occurring most frequently in correspondence of the small airways, and in order to avoid the underestimation of the lumen area.

## 3.3. Quantitative Analysis Of The Airways In Healthy Subjects And Patients With Asthma

The algorithm developed in the present work has been used to quantify the structural alterations occurring in the airways due to asthma. To this aim, the airways have been measured in healthy and asthmatic patients and the results are compared between the two groups. The measurements concerning the right and the left lung are retrieved and analysed. The results are reported both separated (Appendix A) and together for all the morphological parameters considered.

In particular, in Fig. 3.5 are reported the results of the measured lumen area (LA), bronchial wall area (WA) and total area (TA), expressed in $mm^2$, and of the wall percentage area (WA%), expressed in %.

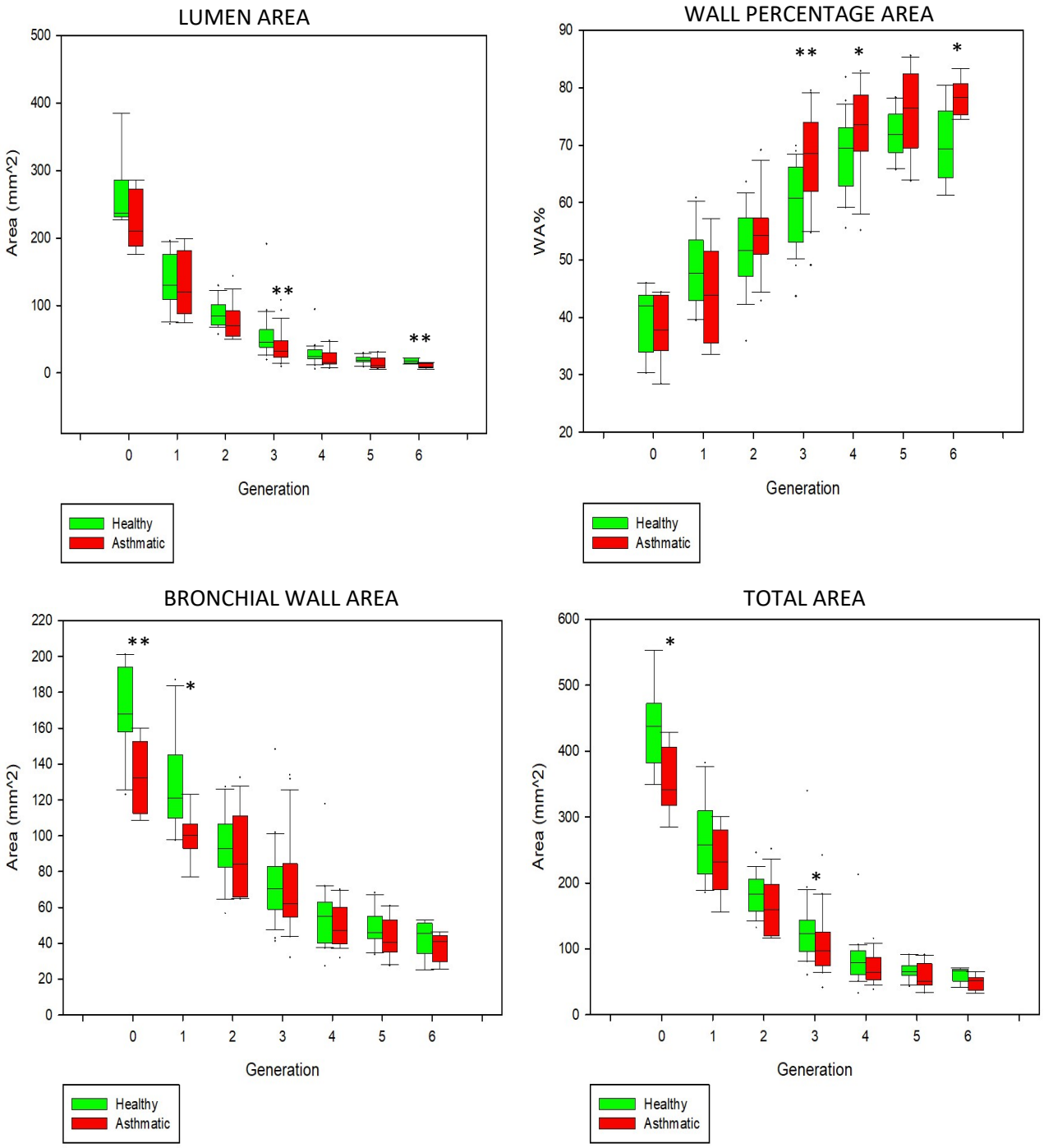


Figure 3.5: Measurements of area: box-plots and statistical analysis represented as * P-value ≤ 0.05, ** P-value ≤ 0.01, *** P-value ≤ 0.001

Lumen area (LA) is lower in patient with asthma than in healthy subjects and a statistical significant difference is found in correspondence of the third and sixth generation, with a p-value equal to 0.007 and 0.004 respectively. Analogous results are found separately considering the right and the left lung. In the right lung, a statistical significant difference is found, also in correspondence of the second and fourth generation. In the left lung, LA in asthmatic patient is lower than the corresponding LA in healthy subjects, with a statistical significant difference just in correspondence of the third generation.

Wall percentage area (WA%) is larger in patient with asthma than in healthy patient, starting from the third generation, with significant differences at the third, fourth, and sixth generation, with a p-value equal to 0.00116, 0.0588, and 0.0172 respectively. Analogous results are found considering the right and the left lungs separately.

Total area (TA) decreases in patients with asthma compared to healthy subjects, and a statistical significant difference is found in correspondence of the zero and third generation, with a p-value equal to 0.012 and 0.015, respectively. Analogous results are found when the left and the right lungs are considered separately.

Concerning the wall area (WA), significant statistical differences are found just in correspondence of the first two generations, with p-values equal to 0.002 and 0.013, respectively. No significant statistical difference is found considering the left and right lung separately.

The comparison of lumen area between healthy and asthmatic subjects can be qualitative evaluated by comparing the segmentation images of the airway lumen, to which a colormap has been associated. The colour and its intensity of each airway segments changes according to the value of lumen area specific for that airway. An example case is reported in Appendix B.

In Fig. 3.6, the measurements of distance are reported, including the wall thickness (WT), the mean inner and outer diameter (respectively ID and OD), expressed in mm, and the ratio between the wall thickness and the mean outer diameter (WT/OD).

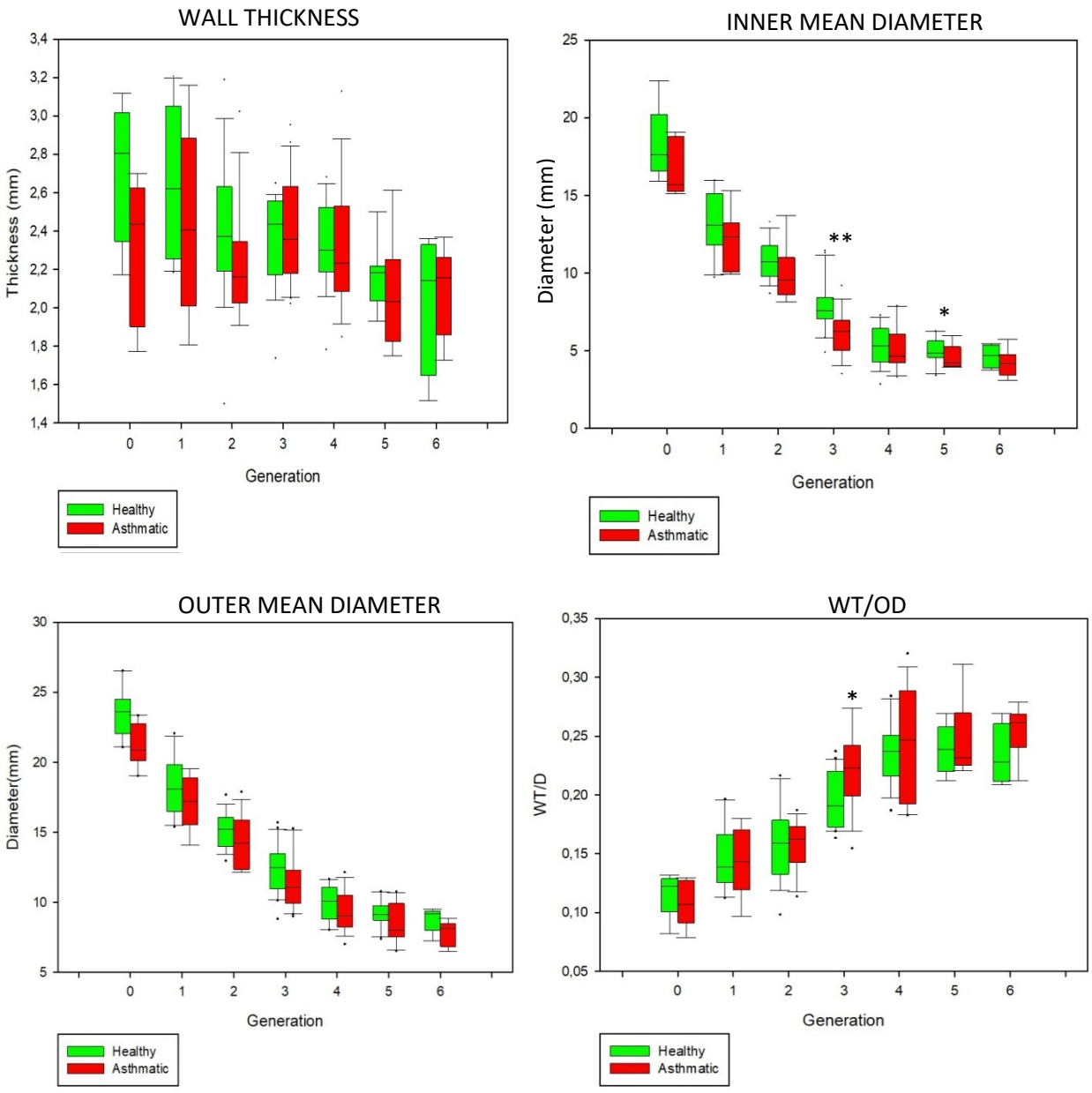


Figure 3.6 Measurements of distance: box-plots and statistical analysis represented as * P-value ≤ 0.05, ** P-value ≤ 0.01, *** P-value ≤ 0.001

No significant statistical difference is found for the wall thickness (WT) and the outer diameter (OD) between the two groups. Similar results are obtained if considering the left lung only, whereas a significant lower WT and OD in the asthmatic group are found in the right lung,.

The mean inner diameter is lower in asthmatic patients from the third generation, with a significant difference between the two groups at the third and fifth generation, with p-value equal to 0.0014 and 0.045, respectively.

WT/OD is greater in asthmatic patients than healthy subjects from the third generation (p-value = 0.0189 at generation 3), with a large variability among the two populations. Considering the left lung only, a statistical difference is found also at the level of the sixth generation, with a p-value equal to 0.0274.

The results related to the measurements of LA and WA% are coherent with the ones obtained from previous works. There is a decrease of LA and an increase of WA% in asthmatic subjects with respect to the healthy ones, in particular from the third generation downwards.

The fact that WA seems to be greater in the healthy than in the asthma group is in contradiction with previously published studies that found either no difference [55] or the opposite phenomenon [29]. Nevertheless, Montaudon et al. [10] found similar results, hypothesizing that WA depends on the bronchial size. Coherently with this theory, in our work, total area is lower in patients with asthma than in healthy subjects, also with a certain statistical significance.

In light of this consideration, also the measurements of the lumen area may be affected by the bronchial size. Therefore, the significant statistical difference found could be caused by the structural change occurring with asthma, but also by the fact that airways of asthmatic patients seem to be smaller compared to healthy.

Instead, WA% is less dependent from the highly variable airway size present among different patients. This represents a valid reason to preferably consider WA% as the most relevant parameter to investigate the structural changes occurring with the disease.

Considering the measurements of distance, WT is not found to be greater in asthmatic patients than in healthy patients, as expected. This result is in contradiction with the ones found in several previous works and also Montaudon et al. [10], even though obtained a smaller WA for asthmatic patient actually found that in each bronchial generation WT tended to be higher in patients with asthma than in healthy subjects.

Our results can be justified considering once again the fact that the total area is lower in asthmatic patients. This is demonstrated also by the graphs of the outer diameter, where lower values are found in asthmatic airways. Indeed, considering WT/OD, the ratio between wall thickness and outer diameter, greater values are found in asthmatic patients than in the healthy. This difference is significant just at the third generation, downwards no significant differences are found and moreover a larger data variability is observable.

In conclusion, airways structural changes are present in patients with asthma. This is demonstrated especially by WA% and WT/OD, which are considered more reliable than the other morphological parameters. The results obtained in this thesis work demonstrates that there is a thickening of the bronchial wall and a lumen narrowing of airways in asthmatic patients. These results suggest that the present tool may provide quantitative imaging biomarkers in pulmonary diseases affecting the airways, for patients' follow-up or to investigate the effect of novel pharmacological treatments.

# 3.4. An Insight Into Structure-Function Relationship In Asthma: A Comparison Between 3He-MRI And CT Images

The tool developed during this work may be used to further investigate the structure-function relationship in pulmonary disease. In this short paragraph we want to show the potentiality of this tool in this field.

Among the patients with asthma, we identified one patient with a signal void in the 3He-MR image, corresponding to a region not reached by 3He. In the corresponding CT image, the WA% and LA/TA are retrieved for the airway close to the region where the abnormality has been identified on 3He-MRI.

The same airway is identified in the CT images of all the healthy subjects, and the mean value of WA% and LA/TA are calculated for comparison.

The region of signal void is identified in the apical part of the left bronchus and so the airway taken into consideration is the one of the left upper lobe and the deepest generation reached is the 4$^{th}$.

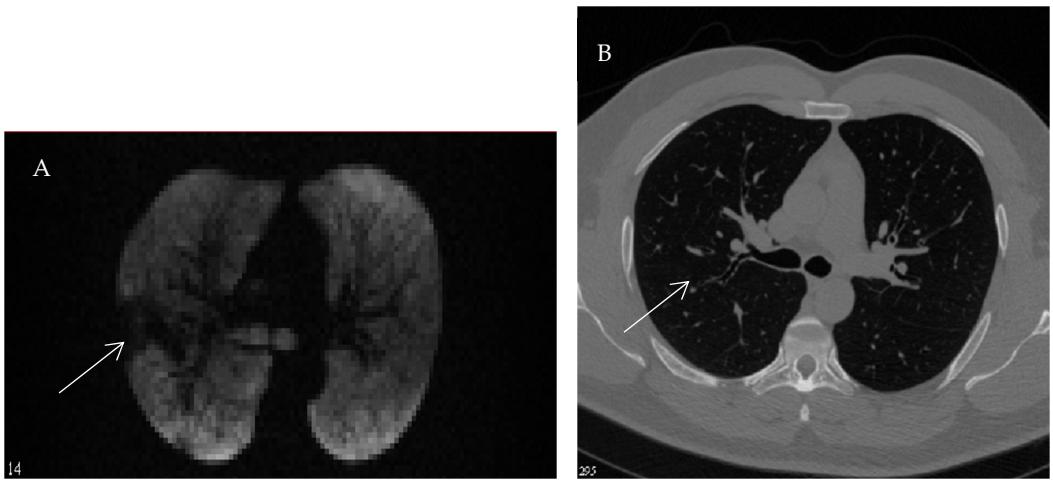


Figure 3.7 A) He3-MRI of asthmatic patient, the white arrow indicates the region of air trapping; B) correspondent slice in the CT image, the white arrow indicates the relevant airway taken into consideration to evaluate the structural changes occurring in correspondence of air trapping.

The corresponding WA% and LA/TA are equal to 80,17% and 19,82% respectively. The analogous airway in the healthy subjects is characterized a mean value of WA% and LA/TA respectively equal to 73,23% and 26,77%.

These values demonstrates a thickening of the bronchial wall and a narrowing of the lumen in that specific airway in this representative asthmatic patient and these structural changes are the responsible for the signal void visible in 3He-MRI.

These representative results suggest that a deeper analysis of the airways may be useful to further investigate the relationship existing between structural alterations of the airways and the functional impairment observed in lung parenchyma. A future study may aim to investigate the correlation between the airways' parameters, calculated with the developed algorithm, and pulmonary ventilation, quantified by 3He-MRI in regions of interest such as lobes or segments. This analysis may also be extended to other lung diseases, such as cystic fibrosis or lung transplantation, in which the relationship between lung function and structural alterations, both of the airways and of the lung parenchyma, is still unclear, but which is fundamental to understand the mechanisms of disease progression and the effect of treatment.

# 4 Conclusion

The objective of the present work of thesis was the development of a new algorithm for the extraction and accurate measurements of morphological airways parameters.

Considering the results thus obtained, it can be concluded that the implemented algorithm is a valid and innovative tool for quantitative airway analysis.

At first a segmentation algorithm is applied to segment the airway lumen. This procedure is qualitative evaluated by a visual inspection, and no leakage of the airways on the lung parenchyma is noticed. Another consideration we can do about the efficiency of this algorithm is that the lumen area, which is directly retrieved from the segmented object by applying the resample procedure, is successfully validated. Just a slight underestimation is detected. This issue can be solved by improving the iterative region growing algorithm adopted for the segmentation procedure. In particular, at each iteration new pixels are set as seeds if their intensity value is lower than a given threshold. So, in a future development of the work, a more suitable value of threshold could be establish to comprise more pixels during the segmentation. Alternatively, another approach adopted by some studies [59][60], is to calculate the lumen area on the 2D grey-scale image obtained by resampling the original CT image, implementing an algorithm both for the inner and outer border detection and calculate at the same time lumen and total area.

The number of generations reached by the segmentation algorithm is found to be lower than in other studies [3][10][27] mainly due to the image processing procedure implemented for obtaining an accurate centreline.

The accurate identification of the centreline from the segmented airway lumen is paramount to accomplish the further steps and analysis.

Indeed, starting from the centreline, the points where make the measurements were retrieved as well as the direction necessary to extract the 2D orthogonal section from the 3D image. Therefore, the accuracy in the measurements depends also on an accuracy in retrieving the centreline.

The extraction of the 2D section allowed to perform the measurements in every airway, and this is a superior approach compared to other studies [24][29] which retrieved measurements just in some region, usually the apical bronchus of the right upper lobe, where the airways run orthogonal with respect to the image plane. Actually a further improvement that should be implemented in a future development of this work is to consider as perpendicular direction, used to extract the 2D orthogonal section of the airways, the tangent to the centreline in the point selected for the measurement[20], instead of calculating the difference between the coordinates of the selected point and the one three position ahead in the centerline. This can potentially improve the accuracy in performing the measurements.

So, in order to obtain a centreline without spurs or defects, a closing filter followed by an opening filter is applied which caused a reduction in the number of generations detected. It is important to develop a tool capable of detecting, and so analyse, a large amount of airways and in the most distal positions, to evaluate the phenomena of airways obstruction and airflow limitation where they are more relevant and serious. An alternative strategy for a correct centreline extraction should be considered, as the one implemented by Ma et al.[58]. A connectivity preserving fully-parallel 3D thinning algorithm was designed to preserve both the geometry of the original object and important details such as small airway bifurcations[57]. The main principle was to erode the volume of the segmented airway lumen from the outermost surface in a layer by layer manner until only a centerline remains. A total

of 38 erosion templates were designed, any voxel that fit one of the templates was removed and, at the same time, preservation conditions were applied to prevent the removal of the end points of airway segments[17].

Moreover, starting from an accurate centreline it was possible to correctly detect the branching (bifurcation) points and create the tree data structure for data organization. The implementation of the tree data structure was another necessary step for the following analysis as allowed to detect and re-build the same hierarchical structure of the trachea-bronchial tree, peculiar for each patient. In particular, it allowed to efficiently perform a suitable labelling, to associate the measurements to its corresponding airway branch and to compare corresponding generations of airways between subjects.

A missing part of this work of thesis is the validation of this process of bifurcation points identification from the centerline. A wrong identification of these points leads to a wrong implementation of the tree data structure, so to a wrong identification of the airway generation, and to a consequent erroneous comparison of corresponding generations between healthy and asthmatic subjects. Previous studies [3][56] validate this step using a gold standard provided by an expert image analyst who would perform manually segmentation or alternatively using phantom studies [17].

Concerning the segmentation of the outer wall border, a simple method consisting on an iterative dilatation process has been implemented and successfully validated. Some erroneous measurements are anyway present but mainly derived from error in detecting the corresponding lumen area. The other morphological parameters, as derived from lumen area and total area, can be considered successfully validate too.

The results obtained from the comparison phase can be considered encouraging. Indeed, asthma is an obstructive pathology characterized by an airflow limitation especially during the exhalation phase, while the data taken into consideration were

CT images acquired in the maximum inspiration phase (TLC)- Nevertheless, significant differences were found between healthy and asthmatic subjects.

Furthermore, even if in the present work asthma is the pathology taken into consideration, the developed algorithm can potentially be applied to other lung diseases that lead to airways' structural changes detectable on CT images, such as pulmonary fibrosis.

Finally, an insight is reported about the structure-function correlation in lung disease that can be potentially assessed using the developed tool and 3He-MRI. What is reported in this work of thesis is just an example case and future studies will further investigate this correlation.

This method also presents some limitations. The number of analized data was limited, so, the implemented algorithm may not be robust enough to take into account for the large variability in shape, number and size of the airways among different individuals and different pulmonary diseases.

Moreover, the validation procedure is done through a comparison with measurements obtained by a manual segmentation. This method typically suffers from a relatively large intra- and inter-variability, in particular considering the small airways, and so may not be considered very reliable [17]. An alternative validation method could consists on comparing measurements with some 'gold standard' related to lung airways that is shared and available to the public.

The road towards a possible clinical application is long and the developed algorithm needs further investigations and improvements. However, in a long-term perspective this method could support diagnosis, follow-up and treatment definition.

# Bibliography

[1] Patwa A, Shah A. Anatomy and physiology of respiratory system relevant to anaesthesia. Indian J Anaesth. 2015 Sep;59(9):533-41. doi: 10.4103/0019-5049.165849. PMID: 26556911; PMCID: PMC4613399.

[2] Mauriello S. Automatic labeling and nomenclature of the tracheo-bronchial tree reconstructed from volumetric CT lung images. Tesi di laurea, Politecnico di Milano, 2009-2010.

[3] Aykac D, Hoffman EA, McLennan G, Reinhardt JM. Segmentation and analysis of the human airway tree from three-dimensional X-ray CT images. IEEE Trans Med Imaging. 2003 Aug;22(8):940-50. doi: 10.1109/TMI.2003.815905. PMID: 12906248.

[5] Mims JW. Asthma: definitions and pathophysiology. Int Forum Allergy Rhinol. 2015 Sep;5 Suppl 1:S2-6. doi: 10.1002/alr.21609. PMID: 26335832.

[6] Quirt J, Hildebrand KJ, Mazza J, Noya F, Kim H. Asthma. Allergy Asthma Clin Immunol. 2018 Sep 12;14(Suppl 2):50. doi: 10.1186/s13223-018-0279-0. PMID: 30275843; PMCID: PMC6157154.

[7] Tagaya E, Tamaoki J. Mechanisms of airway remodeling in asthma. Allergol Int. 2007 Dec;56(4):331-40. doi: 10.2332/allergolint.R-07-152. Epub 2007 Nov 1. PMID: 17965576

[8] Munakata M. Airway remodeling and airway smooth muscle in asthma. Allergol Int. 2006 Sep;55(3):235-43. doi: 10.2332/allergolint.55.235. PMID: 17075263

[9] Bousquet J, Chanez P, Lacoste JY, White R, Vic P, Godard P, Michel FB. Asthma: a disease remodeling the airways. Allergy. 1992 Feb;47(1):3-11. doi: 10.1111/j.1398-9995.1992.tb02242.x. PMID: 1590563

[10] Montaudon M, Lederlin M, Reich S, Begueret H, Tunon-de-Lara JM, Marthan R, Berger P, Laurent F. Bronchial measurements in patients with asthma: comparison of quantitative thin-section CT findings with those in healthy subjects and correlation with pathologic findings. Radiology. 2009 Dec;253(3):844-53. doi: 10.1148/radiol.2533090303. Epub 2009 Sep 29. PMID: 19789219.

[11] Wang D, Luo J, Du W, Zhang LL, He LX, Liu CT. A morphologic study of the airway structure abnormalities in patients with asthma by high-resolution computed

tomography. J Thorac Dis. 2016 Oct;8(10):2697-2708. doi: 10.21037/jtd.2016.09.36. PMID: 27867544; PMCID: PMC5107441.

[12] de Jong PA, Müller NL, Paré PD, Coxson HO. Computed tomographic imaging of the airways: relationship to structure and function. Eur Respir J. 2005 Jul;26(1):140-52. doi: 10.1183/09031936.05.00007105. PMID: 15994401.

[13] Harvey O. Coxson. Lung parenchyma density and airwall thickness in airway diseases. Breathe 2012 9: 36-45; DOI: 10.1183/20734735.018912

[14] Hermena S, Young M. CT-scan Image Production Procedures. 2022 Aug 8. In: StatPearls [Internet]. Treasure Island (FL): StatPearls Publishing; 2022 Jan–. PMID: 34662062.

[15] Walker C, Gupta S, Hartley R, Brightling CE. Computed tomography scans in severe asthma: utility and clinical implications. Curr Opin Pulm Med. 2012 Jan;18(1):42-7. doi: 10.1097/MCP.0b013e32834db255. PMID: 22112997; PMCID: PMC3387553.

[16] Wang D, Luo J, Du W, Zhang LL, He LX, Liu CT. A morphologic study of the airway structure abnormalities in patients with asthma by high-resolution computed tomography. J Thorac Dis. 2016 Oct;8(10):2697-2708. doi: 10.21037/jtd.2016.09.36. PMID: 27867544; PMCID: PMC5107441.

[17] Pu J, Gu S, Liu S, Zhu S, Wilson D, Siegfried JM, Gur D. CT based computerized identification and analysis of human airways: a review. Med Phys. 2012 May;39(5):2603-16. doi: 10.1118/1.4703901. PMID: 22559631; PMCID: PMC3344883.

[18] Fabijańska A. Two-pass region growing algorithm for segmenting airway tree from MDCT chest scans. Comput Med Imaging Graph. 2009 Oct;33(7):537-46. doi: 10.1016/j.compmedimag.2009.04.012. Epub 2009 May 26. PMID: 19473814.

[19] Grenier PA, Fetita CI, Brillet PY. Quantitative computed tomography imaging of airway remodeling in severe asthma. Quant Imaging Med Surg. 2016 Feb;6(1):76-83. doi: 10.3978/j.issn.2223-4292.2016.02.08. PMID: 26981458; PMCID: PMC4775245.

[20] Tschirren J, Hoffman EA, McLennan G, Sonka M. Intrathoracic airway trees: segmentation and airway morphology analysis from low-dose CT scans. IEEE Trans Med Imaging. 2005 Dec;24(12):1529-39. doi: 10.1109/TMI.2005.857654. PMID: 16353370; PMCID: PMC1851666.]

[21] Hackx M, Bankier AA, Gevenois PA. Chronic obstructive pulmonary disease: CT quantification of airways disease. Radiology. 2012 Oct;265(1):34-48. doi: 10.1148/radiol.12111270. PMID: 22993219.

[22] San José Estépar R, Reilly JJ, Silverman EK, Washko GR. Three-dimensional airway measurements and algorithms. Proc Am Thorac Soc. 2008 Dec 15;5(9):905-9. doi: 10.1513/pats.200809-104QC. PMID: 19056714.

[24] Patyk M, Obojski A, Sokołowska-Dąbek D, Parkitna-Patyk M, Zaleska-Dorobisz U. Airway wall thickness and airflow limitations in asthma assessed in quantitative computed tomography. Ther Adv Respir Dis. 2020 Jan-Dec;14:1753466619898598. doi: 10.1177/1753466619898598. PMID: 31964312; PMCID: PMC6977202.

[25] Ranu H, Wilde M, Madden B. Pulmonary function tests. Ulster Med J. 2011 May;80(2):84-90. PMID: 22347750; PMCID: PMC3229853.

[26] Davidson KR, Ha DM, Schwarz MI, Chan ED. Bronchoalveolar lavage as a diagnostic procedure: a review of known cellular and molecular findings in various lung diseases. J Thorac Dis. 2020 Sep;12(9):4991-5019. doi: 10.21037/jtd-20-651. PMID: 33145073; PMCID: PMC7578496.

[27] Aysola R, de Lange EE, Castro M, Altes TA. Demonstration of the heterogeneous distribution of asthma in the lungs using CT and hyperpolarized helium-3 MRI. J Magn Reson Imaging. 2010 Dec;32(6):1379-87. doi: 10.1002/jmri.22388. PMID: 21105142.

[28] Gaeta, M., Minutoli, F., Girbino, G. et al. Expiratory CT scan in patients with normal inspiratory CT scan: a finding of obliterative bronchiolitis and other causes of bronchiolar obstruction. Multidiscip Respir Med 8, 44 (2013). https://doi.org/10.1186/2049-6958-8-44

[29] Niimi A, Matsumoto H, Amitani R, Nakano Y, Mishima M, Minakuchi M, Nishimura K, Itoh H, Izumi T. Airway wall thickness in asthma assessed by computed tomography. Relation to clinical indices. Am J Respir Crit Care Med. 2000 Oct;162(4 Pt 1):1518-23. doi: 10.1164/ajrccm.162.4.9909044. PMID: 11029371.

[30 ] Hoshino M, Matsuoka S, Handa H, Miyazawa T, Yagihashi K. Correlation between airflow limitation and airway dimensions assessed by multidetector CT in asthma. Respir Med. 2010 Jun;104(6):794-800. doi: 10.1016/j.rmed.2009.12.005. Epub 2010 Jan 6. PMID: 20053544.

[31] Kasahara K, Shiba K, Ozawa T, Okuda K, Adachi M. Correlation between the bronchial subepithelial layer and whole airway wall thickness in patients with

asthma. Thorax. 2002 Mar;57(3):242-6. doi: 10.1136/thorax.57.3.242. PMID: 11867829; PMCID: PMC1746264.

[32] Berair R, Hartley R, Mistry V, Sheshadri A, Gupta S, Singapuri A, Gonem S, Marshall RP, Sousa AR, Shikotra A, Kay R, Wardlaw A, Bradding P, Siddiqui S, Castro M, Brightling CE. Associations in asthma between quantitative computed tomography and bronchial biopsy-derived airway remodelling. Eur Respir J. 2017 May 1;49(5):1601507. doi: 10.1183/13993003.01507-2016. PMID: 28461289; PMCID: PMC5744590.

[33] Fain SB, Gonzalez-Fernandez G, Peterson ET, Evans MD, Sorkness RL, Jarjour NN, Busse WW, Kuhlman JE. Evaluation of structure-function relationships in asthma using multidetector CT and hyperpolarized He-3 MRI. Acad Radiol. 2008 Jun;15(6):753-62. doi: 10.1016/j.acra.2007.10.019. PMID: 18486011; PMCID: PMC2744977.

[34] Lauri H. High-resolution CT of the lungs: Indications and diagnosis. Duodecim. 2017;133(6):549-56. PMID: 29243467.

[35] Tsurikisawa N, Oshikata C, Tsuburai T, Saito H, Sekiya K, Tanimoto H, Takeichi S, Mitomi H, Akiyama K. Bronchial hyperresponsiveness to histamine correlates with airway remodelling in adults with asthma. Respir Med. 2010 Sep;104(9):1271-7. doi: 10.1016/j.rmed.2010.03.026. Epub 2010 Apr 24. PMID: 20418085.

[36] Cohen L, E X, Tarsi J, et al. Epithelial cell proliferation contributes to airway remodeling in severe asthma. Am J Respir Crit Care Med 2007;176:138–145.

[37] Holmes JH, O'Halloran RL, Brodsky EK, et al. Three-dimensional imaging of ventilation dynamics in asthmatics using multiecho projection acquisition with constrained reconstruction. MagnReson Med 2009;62:1543–1556.

[38] Halder A, Chatterjee S, Dey D, Kole S, Munshi S. An adaptive morphology based segmentation technique for lung nodule detection in thoracic CT image. Comput Methods Programs Biomed. 2020 Dec;197:105720. doi: 10.1016/j.cmpb.2020.105720. Epub 2020 Aug 25. PMID: 32877818.

[39] M. C. Clark, L. O. Hall, D. B. Goldgof, R. Velthuizen, F. R. Murtagh and M. S. Silbiger, "Automatic tumor segmentation using knowledge-based techniques," in IEEE Transactions on Medical Imaging, vol. 17, no. 2, pp. 187-201, April 1998, doi: 10.1109/42.700731.

[40] Nadeem SA, Hoffman EA, Sieren JC, Comellas AP, Bhatt SP, Barjaktarevic IZ, Abtin F, Saha PK. A CT-Based Automated Algorithm for Airway Segmentation

Using Freeze-and-Grow Propagation and Deep Learning. IEEE Trans Med Imaging. 2021 Jan;40(1):405-418. doi: 10.1109/TMI.2020.3029013. Epub 2020 Dec 29. PMID: 33021934; PMCID: PMC7772272.

[41] Han Y. Reliable Template Matching for Image Detection in Vision Sensor Systems. Sensors (Basel). 2021 Dec 7;21(24):8176. doi: 10.3390/s21248176. PMID: 34960270; PMCID: PMC8706661.

[42] McCormick M, Liu X, Jomier J, Marion C, Ibanez L. ITK: enabling reproducible research and open science. Front Neuroinform. 2014;8:13. Published 2014 Feb 20. doi:10.3389/fninf.2014.00013

[43] Yoo TS, Ackerman MJ, Lorensen WE, Schroeder W, Chalana V, Aylward S, Metaxas D, Whitaker R. Engineering and Algorithm Design for an Image Processing API: A Technical Report on ITK – The Insight Toolkit. In Proc. of Medicine Meets Virtual Reality, J. Westwood, ed., IOS Press Amsterdam pp 586-592 (2002).

[44] Van der Walt S, Sch"onberger, Johannes L, Nunez-Iglesias J, Boulogne, Franccois, Warner JD, Yager N, et al. scikit-image: image processing in Python. PeerJ. 2014;2:e453.

[45] Juan Nunez-Iglesias, Adam J. Blanch, Oliver Looker, Matthew W. Dixon, and Leann Tilley. A new Python library to analyse skeleton images confirms malaria parasite remodelling of the red blood cell membrane skeleton. *PeerJ*, 6:e4312, 2018. doi:10.7717/peerj.4312.

[46] Nadeem SA, Hoffman EA, Comellas AP, Saha PK. Anatomical Labeling of Human Airway Branches using a Novel Two-Step Machine Learning and Hierarchical Features. Proc SPIE Int Soc Opt Eng. 2020 Feb;11313:1131312. doi: 10.1117/12.2546004. Epub 2020 Mar 10. PMID: 34267414; PMCID: PMC8279009.

[47] Williamson JP, James AL, Phillips MJ, Sampson DD, Hillman DR, Eastwood PR. Quantifying tracheobronchial tree dimensions: methods, limitations and emerging techniques. Eur Respir J. 2009 Jul;34(1):42-55. doi: 10.1183/09031936.00020408. PMID: 19567601.

[48] Mueller D. "LookAt Transform Initializer and Oblique Section Image Filter". The Insight Journal. 2007 lug. http://hdl.handle.net/1926/563

[49] World Health Organization. (2016). Ambient air pollution: a global assessment of exposure and burden of disease. World Health Organization

[50] Masoli M, Fabian D, Holt S, Beasley R; Global Initiative for Asthma (GINA) Program. The global burden of asthma: executive summary of the GINA

Dissemination Committee report. Allergy. 2004 May;59(5):469-78. doi: 10.1111/j.1398-9995.2004.00526.x. PMID: 15080825.

[51] Devine JF. Chronic obstructive pulmonary disease: an overview. Am Health Drug Benefits. 2008 Sep;1(7):34-42. PMID: 25126252; PMCID: PMC4106574.

[52] Bergeron C, Tulic MK, Hamid Q. Airway remodelling in asthma: from benchside to clinical practice. Can Respir J. 2010 Jul-Aug;17(4):e85-93. doi: 10.1155/2010/318029. PMID: 20808979; PMCID: PMC2933777.

[53] Bergeron C, Tulic MK, Hamid Q. Tools used to measure airway remodelling in research. Eur Respir J. 2007 Mar;29(3):596-604. doi: 10.1183/09031936.00019906. PMID: 17329494.

[54] Fain S, Schiebler ML, McCormack DG, Parraga G. Imaging of lung function using hyperpolarized helium-3 magnetic resonance imaging: Review of current and emerging translational methods and applications. J Magn Reson Imaging. 2010 Dec;32(6):1398-408. doi: 10.1002/jmri.22375. PMID: 21105144; PMCID: PMC3058806.

[55] Aysola RS, Hoffman EA, Gierada D, et al. Airway remodeling measured by multidetector computed tomography is increased in severe asthma and correlates with pathology. Chest 2008;134:1183–1191.

[56] Tschirren J, McLennan G, Palágyi K, Hoffman EA, Sonka M. Matching and anatomical labeling of human airway tree. IEEE Trans Med Imaging. 2005 Dec;24(12):1540-7. doi: 10.1109/TMI.2005.857653. PMID: 16353371; PMCID: PMC2077841.

[57] Chaturvedi A, Lee Z. Three-dimensional segmentation and skeletonization to build an airway tree data structure for small animals. Phys Med Biol. 2005 Apr 7;50(7):1405-19. doi: 10.1088/0031-9155/50/7/005. Epub 2005 Mar 16. PMID: 15798332.

[58] Ma C M and Sonka M 1996 A fully parallel 3D thinning algorithm and its applications Comput. Vis. Image Underst.64 420–33

[59] Tschirren J, Hoffman EA, McLennan G, Sonka M. Segmentation and quantitative analysis of intrathoracic airway trees from computed tomography images. Proc Am Thorac Soc. 2005;2(6):484-7, 503-4. doi: 10.1513/pats.200507-078DS. PMID: 16352753; PMCID: PMC2713337.

[60] Xu Z, Bagci U, Foster B, Mansoor A, Udupa JK, Mollura DJ. A hybrid method for airway segmentation and automated measurement of bronchial wall thickness on CT. Med Image Anal. 2015 Aug;24(1):1-17. doi: 10.1016/j.media.2015.05.003. Epub 2015 May 14. PMID: 26026778; PMCID: PMC4532577.

[61] "Gross Anatomy of the Airway and Lungs: Conducting & Respiratory Zones." Study.com, 7 March 2013, study.com/academy/lesson/gross-anatomy-of-the-airway-and-lungs-conducting-respiratory-zones.html

[62] Sobiesk JL, Munakomi S. Anatomy, Head and Neck, Nasal Cavity. [Updated 2022 Jul 25]. In: StatPearls [Internet]. Treasure Island (FL): StatPearls Publishing; 2023 Jan-.

[63] Suárez-Quintanilla J, Fernández Cabrera A, Sharma S. Anatomy, Head and Neck: Larynx. [Updated 2022 Sep 5]. In: StatPearls [Internet]. Treasure Island (FL): StatPearls Publishing; 2023 Jan-.

**SITOGRAPHY**:

[a] https://quizlet.com/530038751/chapter-23-anatomy-and-physiology-flash-cards/

[b] https://courses.lumenlearning.com/suny-ap2/chapter/the-lungs/

[c] https://www.kenhub.com/en/library/anatomy/the-trachea

[d] https://www.alamy.com/stock-photo/bronchial-tree.html?sortBy=relevant

[e] https://www.pinterest.it/pin/859061697656256190/

[f] https://study.com/academy/lesson/alveolar-ducts-function-definition.html

[g] https://thoracickey.com/functional-anatomy-of-the-respiratory-tract

[h] https://www.fondoasim.it/patologie-polmonari-ostruttive-restrittive

[i] https://www.amherstpeds.com/asthma

[l]https://www.nibib.nih.gov/science-education/science-topics/computed-tomography-ct

[m] https://www.sciencedirect.com/topics/engineering/grayscale-level

[n] https://radiopaedia.org/articles/

[o]https://www.asthma.com/understanding-asthma/what-is-asthma/types-of-asthma/

[p]https://www.healthychildren.org/English/health-issues/conditions/allergies-asthma/Pages/Mild-Moderate-Severe-Asthma-What-Do-Grades-Mean.aspx

[q] https://www.mayoclinic.org/tests-procedures/bronchoscopy/about/pac-20384746

[r] https://www.geeksforgeeks.org/data-structures/

[s] https://www.javatpoint.com/tree

[t] https://skeletonanalysis.org/stable/getting_started/getting_started.html

[u] https://treelib.readthedocs.io/en/latest/index.html

[v] https://mipav.cit.nih.gov/

[z] https://www.ncbi.nlm.nih.gov/books/NBK538202/

# Appendix

**APPENDIX A:**

In this appendix are reported the result of the comparison between healthy and asthmatic subjects considering the data related to right and left lung separately.

Right Lung:

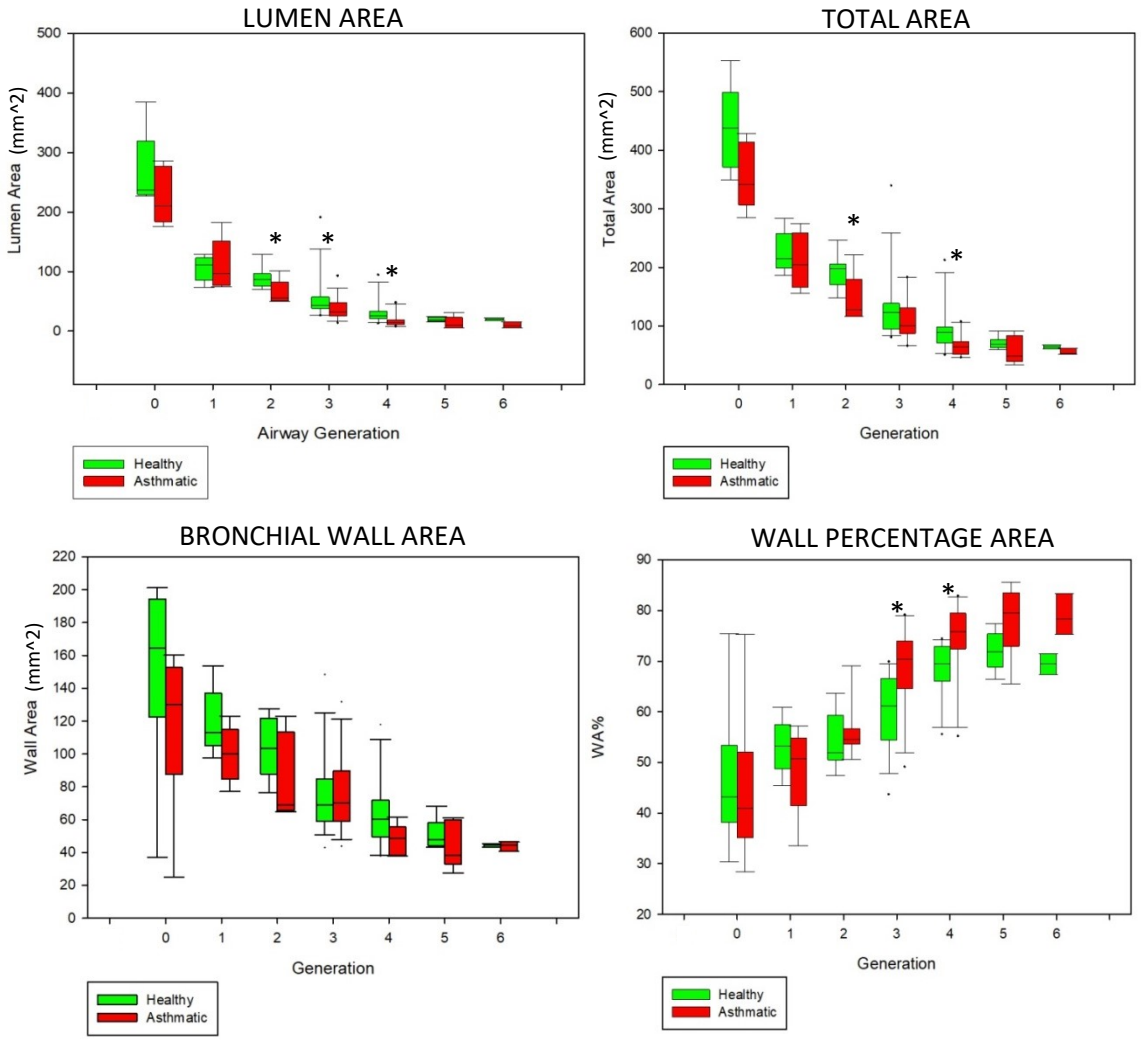


Lumen area in asthmatic patient is lower than in healthy subject and a significant statistical difference is found in correspondence of the second, third and fourth generation with a p-value equal to 0.038, 0.023 and 0.012 respectively.

Also total area in asthmatic patient is lower than in healthy subject and a significant statistical difference is found at the second and fourth generation with a p-value equal to 0.023 and 0.038 respectively.

Concerning the bronchial wall area a great variability of data is observed and no significant statistical difference is found for any generation.

Wall percentage area in asthmatic patient is greater than in healthy subject and a significant statistical difference is found at the third and fourth generation with a p-value equal to 0.012 and 0.018 respectively.

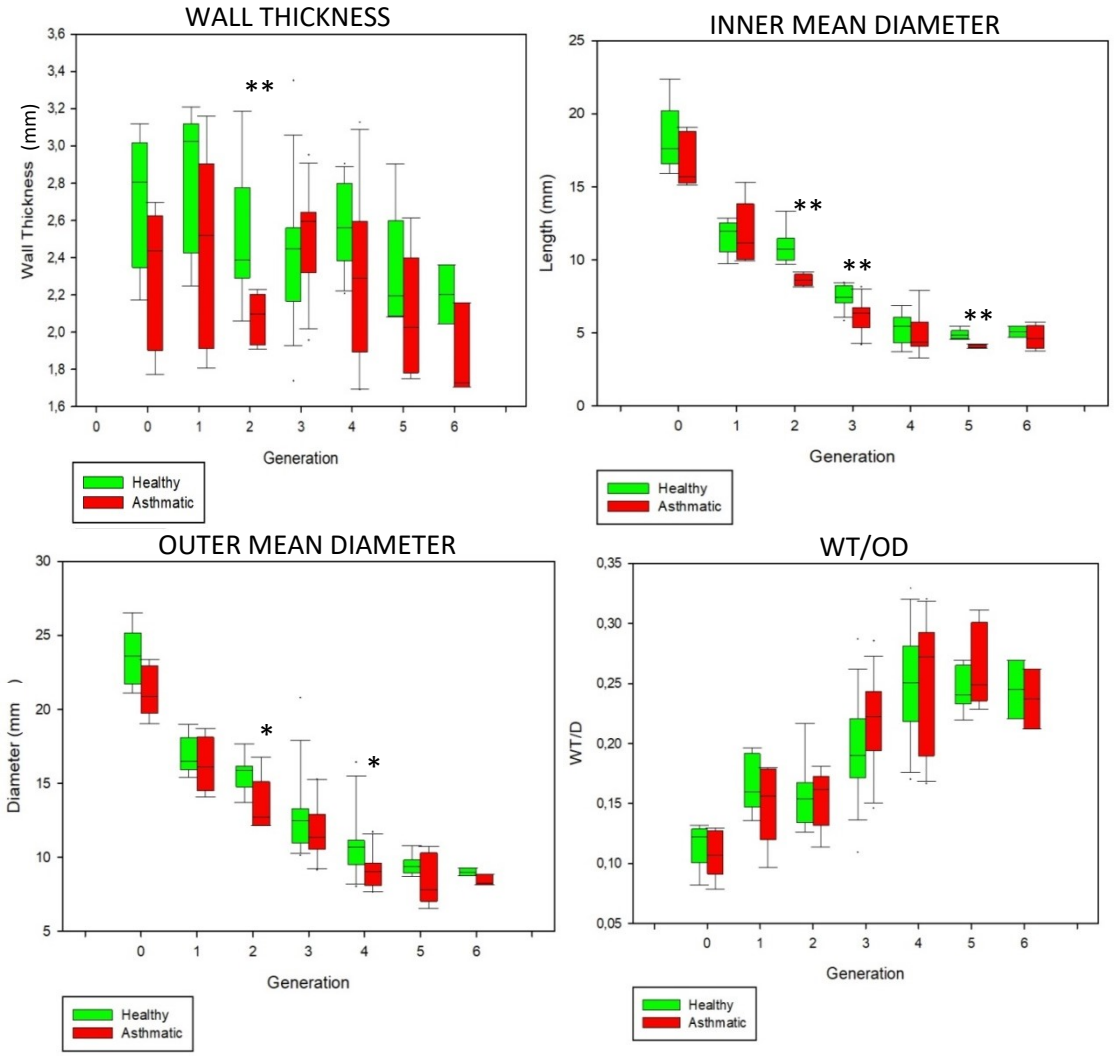


Concerning the wall thickness a great variability among data is observed. A significant statistical difference is found only at the second generation with a lower value for the asthmatic and a p-value equal to 0.005.

The inner mean diameter is lower in asthmatic than in healthy subjects, significant statistical differences are found at the second, third and fifth generation with p-value equal to 0.003, 0.004, 0.002.

The outer mean diameter is lower in asthmatic than in healthy subjects, significant statistical differences are found at the second, third and fifth generation with p-value equal to 0.019 and 0.038 respectively.

Concerning the ratio between wall thickness and outer mean diameter a great variability of data is observed and no significant statistical difference is found.

Left Lung:

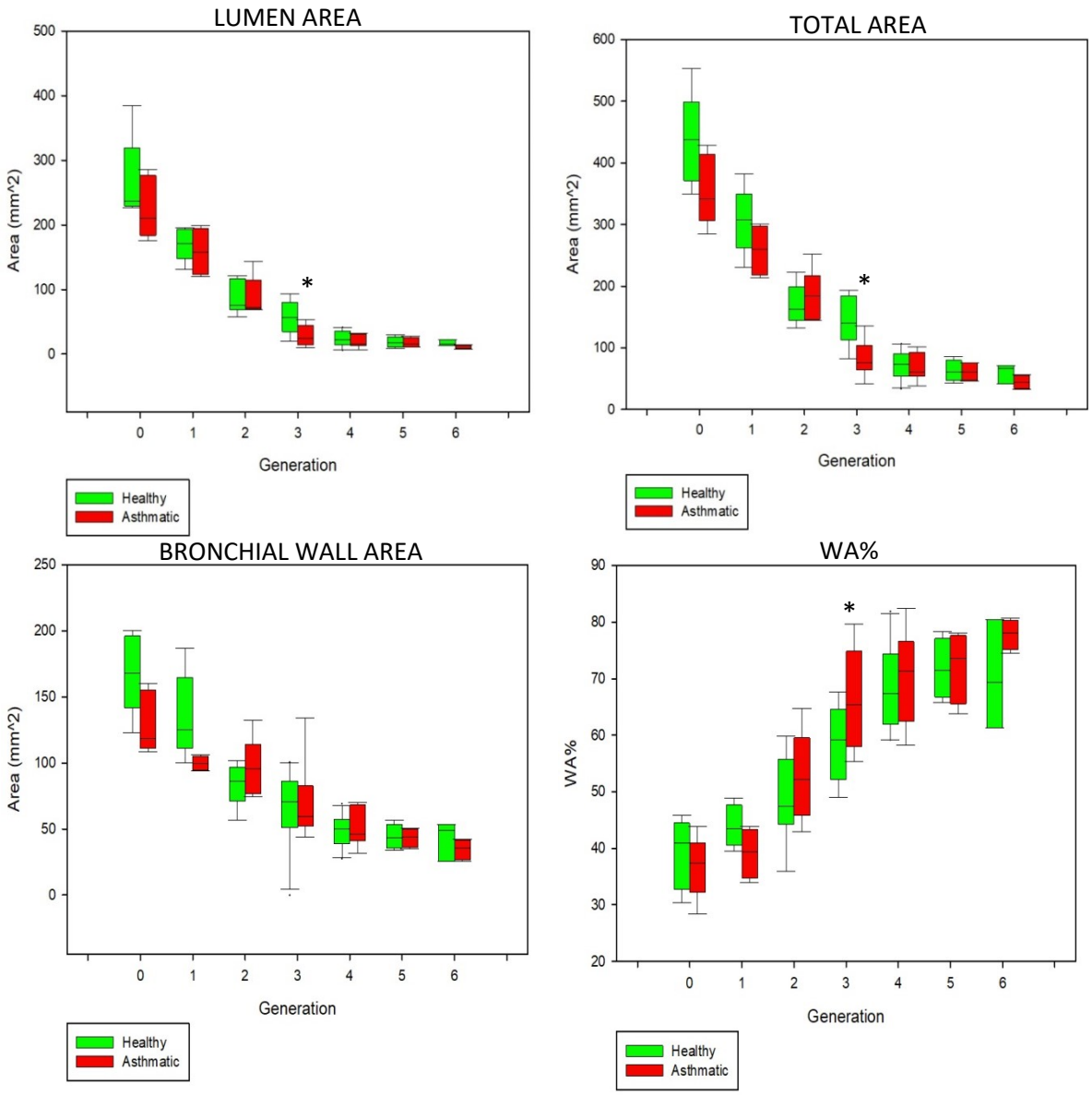

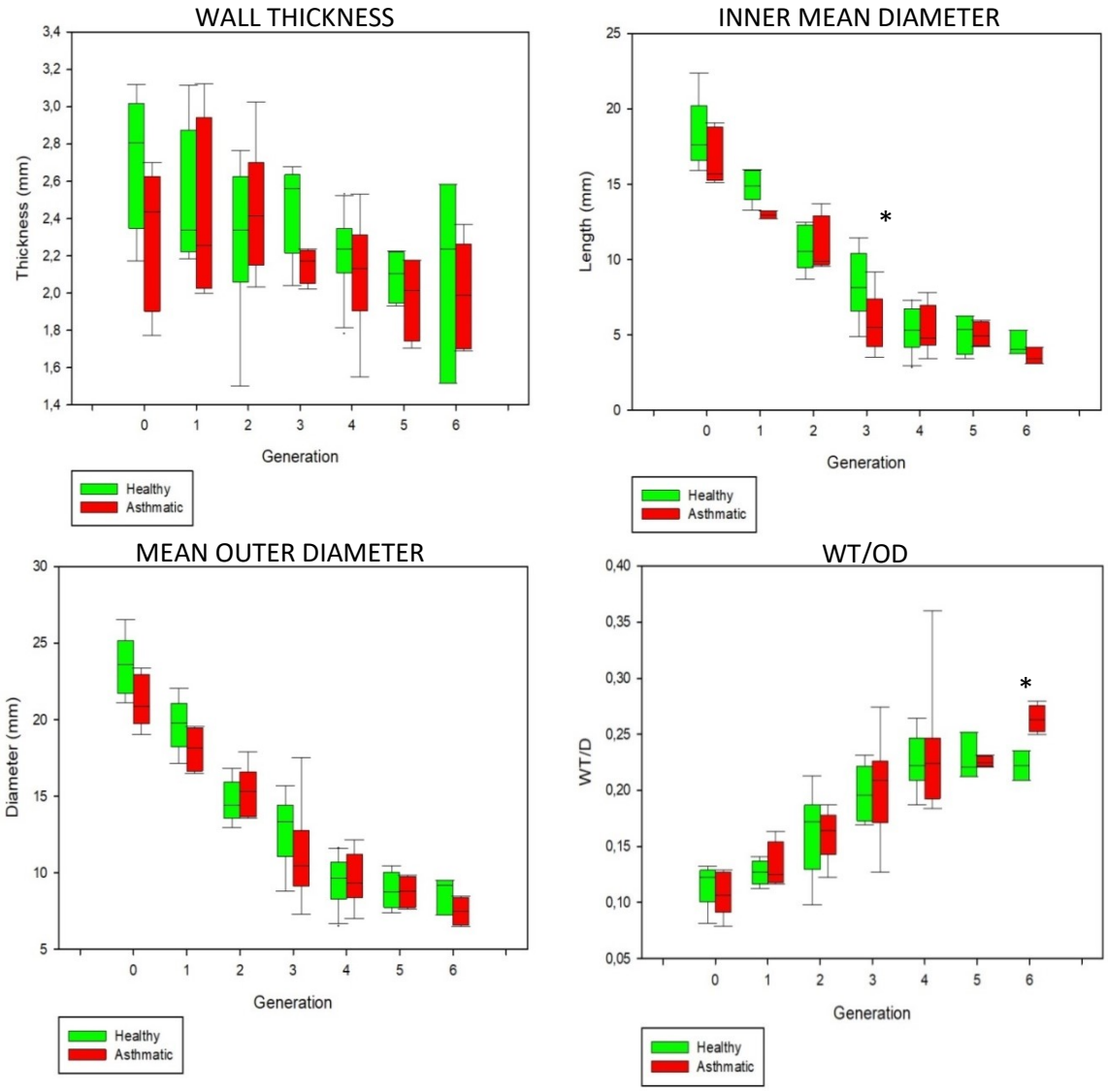


Considering the measurements of distance, in general a great variability of data is observed. The inner mean diameter is lower in asthmatic than in healthy just in the third generation with a p-value equal to 0.047. The ratio WT/OD is lower in asthmatic than in healthy just in the sixth generation with a p-value equal to 0.027. Considering the wall thickness and the mean outer diameter no significant statistical difference is found in any generation.

**APPENDIX B:**

Example of two images represented the result of the airways' lumen segmentation to which a colormap has been associated. One image (left) represents one healthy subjects, the other (right) one asthmatic.

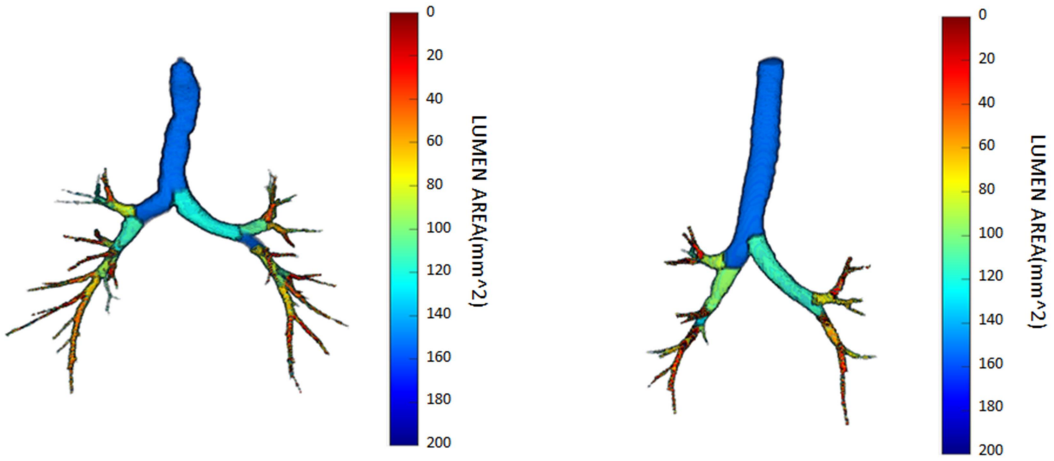

# Abbreviations

LA = Lumen Area

TA = Total Area

WA = Bronchial Wall Area

WA% = Wall Area Percentage

WT = Wall Thickness

OD = Mean Outer Diameter

RMB = Right Main Bronchus

RUL = Right Upper Lobe

BronchInt = Intermediated Bronchus

RML = Right Middle Lobe

RLL = Right Lower Lobe

LMB = Left Main Bronchus

LUL = Left Upper Lobe

LLL = Left Lower Lobe

FEV1 = Forced Expiratory Volume in 1 second

FVC = Forced Vital Capacity

TLC = Total Lung Capacity

# List of Figures